Computational Analysis to Evaluate the Effects of Knee Brace on Anterior Cruciate Ligament during Single-Leg Jump Landing

by

Pratishtha Gupta

A thesis
presented to the University of Waterloo
in fulfillment of the
thesis requirement for the degree of
Master of Applied Science
in
Mechanical and Mechatronics Engineering

Waterloo, Ontario, Canada, 2022

Author's Declaration

I hereby declare that I am the sole author of this thesis. This is a true copy of the thesis, including any required final revisions, as accepted by my examiners.

I understand that my thesis may be made electronically available to the public.

Abstract

Injury and musculoskeletal diseases in the knee due to excessive loading at the ligaments can cause mechanical instability to the joint. Knee bracing has been commonly used to support and provide external stabilization to the joint by restraining its motion and redistributing loads acting on the ligaments. Several studies have been conducted to quantify the effectiveness of knee braces in ligament injury prevention during static and quasi-static loading conditions. However, studies to assess them in dynamic loading conditions remain limited.

The aim of this study was to determine the effects of the mechanical design of a cable stabilized knee brace, inspired by Stoko, on the strain behaviour of the Anterior Cruciate Ligament (ACL) in dynamic loading conditions computationally using Finite Element (FE) analysis. The knee brace evaluated in the current study utilizes a compliant design that has a system of non-extensible pre- tensioned cables running through a compression tight along designed pathways to stabilize the knee mechanics. An FE model of the knee brace was developed on an existing FE model of a knee. The FE model was validated in quasi-static varus/valgus loading conditions by comparing the effective load reduction at the knee to experimental test data available. Single-leg jump landing simulations were then conducted in braced configuration by inputting the muscle forces and joint kinematic/kinetic profiles for ten participants. ACL strain behaviours for post-ground contact duration of 200ms were compared between braced and unbraced configurations to assess the efficacy of knee brace in reducing ligament injury.

The results showed that the effective load at the knee reduced with the brace compared to without the brace during quasi-static varus/valgus loading, similar to the experimental results. Load reduction in braced configuration compared to unbraced configuration was 4.15% during valgus and 29.3% during varus loading condition. During the jump-landing activity, the mean ACL strain in braced configuration increased to 6.59 $\pm$2.41% from 5.54 $\pm$2.41% ($p = 0.024$) in unbraced configuration. The mean time taken for ACL to peak decreased from 80.66 $\pm$27.14 ms in unbraced configuration to 61.33 $\pm$24.61 ms ($p = 0.007$) in braced configuration. It was concluded that the mechanical design of the knee brace could cause the ACL strain to increase during dynamic loading. However, further studies are necessary to evaluate the changes in muscle firing patterns in the braced configuration, their effect on ACL strain behaviour and the effect of knee brace on other knee ligaments such as the Medial Collateral Ligament and Lateral Collateral Ligament.

Acknowledgements

I would first like to thank my supervisor, Dr.Naveen Chandrashekar for providing me with this opportunity to pursue Master's in the field of Biomechanics and work on an impactful project in the Structural Biomechanics Lab at University of Waterloo. I am thankful to him for his constant guidance and support throughout the research project. I want to thank our industry collaborators Stoko for providing us with their K1 Knee Brace and the inducement for this project, especially the R&D Team at Stoko for providing us with the necessary support to complete this study. My sincere thanks to Ryan Bakker for helping me understand more about knee braces and patiently offering advice.

I am grateful to Harish Rao for always helping me with my queries and offering his expertise on any issues that I faced. Thanks to Mercy Ombogo and Raj Arjun Srinivasappa for being great research fellows and helping me with all my queries throughout, but more importantly being great friends.

I also want to thank MITACS for the Globalink Graduate Fellowship and the University of Waterloo for the International Masters Award of Excellence which was immensely helpful in completing my Master's degree. Thanks to Devani Charities for the award that helped me kick-start my move to Canada.

I am immensely grateful for my parents and family for their constant support and encouragement that helped me take on this amazing journey and survive it. Thanks to my friends for always being there for lifting my spirits and continually supporting me.

Table of Contents

List of Figures

List of Tables

Chapter 1

Introduction

1.1 Motivation

Injuries to the knee are one of the most common injuries sustained by the human body. 39.8% of the total sports injuries documented by Majewski et al. (2006) were related to the knee joint. Among these, the most common injury was to the Anterior Cruciate Ligament (ACL) which accounted for 20.3% of the knee injuries during sports activities that require pivoting, cutting or large impact loadings such as soccer, skiing and tennis Majewski et al. (2006). ACL is one of the ligaments of the knee that help provide stability to the knee during complex activities. It can have disrupt and impair the functioning leading to an early onset of degeneration in the knee joint Gerami et al. (2022). Numerous researchers have tried to understand the mechanisms of ACL injury. They are reported to occur in the adolescent and females at a much greater rate than mature males Hewett et al. (2016). In cases of severe injury to the ligament, ACL reconstruction becomes essential for functioning of the knee joint. ACL reconstruction (ACLR) surgeries haven been estimated to be more than 1.5 million in North America since 1980, with an estimated cost of ACLR surgeries being 3 billion USD every year. However, several studies have identified the risk of osteoarthritis in individuals who have undergone ACLR surgery Deacon et al. (1997).

Knee bracing has been employed as an effective technique for knee joint rehabilitation and preventing injuries by providing mechanical stabilization to the knee externally. However, there is no common consensus on the effectiveness of the knee braces in preventing ligament injuries during dynamic loading conditions Najibi and Albright (2005).

Several researchers have tried to answer this question by employing in-vivo and in-vitro methods experimentally. Experimental analysis have their inherent challenges, making

them strenuous. Hence the use of computational method was explored to evaluate the effect of the knee brace on ACL behaviour in dynamic loading conditions. Development of FE model of the knee brace could help predict behaviours of ligaments of interest accurately in both static and dynamic conditions.

1.2 Thesis Objectives

The primary objectives of the current study are summarized below:

1. Develop FE model of cable stabilized brace inspired by Stoko on an existing anatomically accurate knee model developed by Rao (2020).

2. Validate developed model in quasi-static loading condition by comparing the load reduction at the knee with the available experimental data conducted by Stoko in-house using the Knee Testing Fixture and a surrogate leg model.

3. Simulate single-leg jump landings of ten participants with the use of boundary conditions from Bakker (2014) to determine the change in ACL behavior with and without the application of knee brace.

Chapter 2

Background

2.1 Anatomical Background

To clearly describe the human body and the positions of different anatomical locations and their motions relative to each other, a background in the anatomy of the human body is necessary. The following section describes the commonly used anatomical terms and the anatomy of the knee.

2.1.1 Human Anatomical Terms

To describe the motions of different parts of the body, three planes are used as a reference, as shown in Figure 2.1. These are the sagittal/median plane, transverse/horizontal plane and the frontal/coronary plane. The sagittal plane divides the body into right and the left side, the transverse plane into the upper and lower half of the body and the frontal plane into front and back of the body. To define the direction of motion relative to these planes, certain pairs of direction are used as listed below.

- Anterior and posterior - towards the front and the back
- Superior and inferior - towards the head and the limbs
- Medial and lateral - towards and away from the sagittal plane
- Distal and proximal – towards and away from the end of the limbs

Motions of the upper and the lower limbs occurring in the reference planes are described as the following: flexion/extension occurring in the sagittal plane, adduction/abduction in the frontal plane and internal/external rotation in the transverse plane.

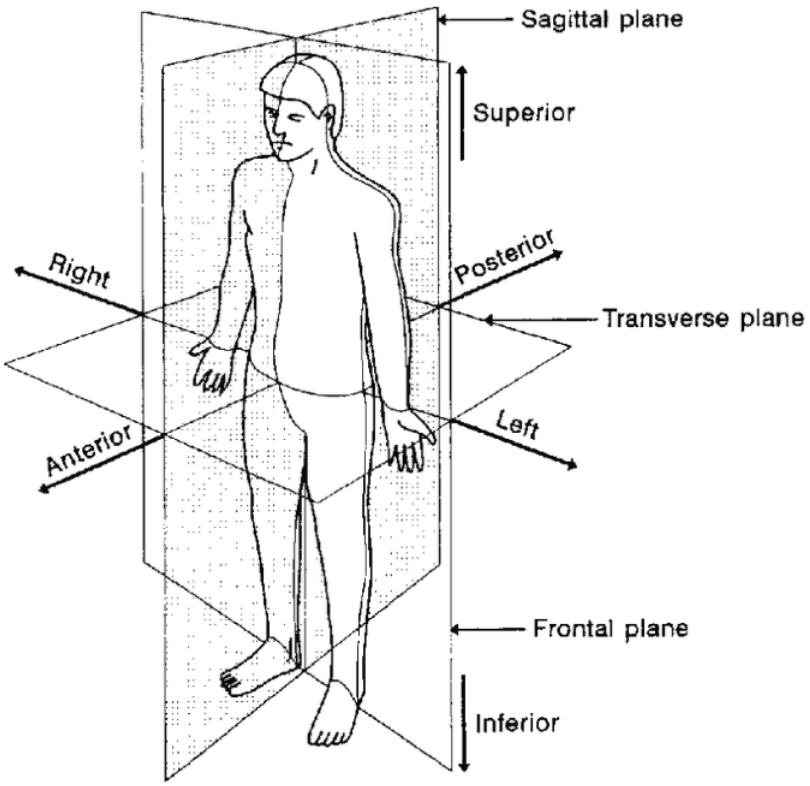

Figure 2.1: Anatomical planes and directions (Adapted from Srinivasan and Sujatha (2022))

2.1.2 Knee Anatomy

The knee joint in the lower limb is the largest synovial joint and the most sophisticated joint in the human body. Its movement is mainly in the sagittal plane for flexion and extension along with some gliding and rotation when in flexion. The knee joint consists of the femur, tibia, patella and the fibula bones (Figure 2.2). Two joint interfaces come together to make the knee joint. These are the tibiofemoral and the patellofemoral joints based on the relative motions of the tibia-femur and patella-femur bones respectively. The tibiofemoral joint supports the axial loading experienced due to the reaction forces of the body weight. The patellofemoral joint acts like a lever to increase the quadriceps muscle force by increasing the length of its moment arm. The stability in these joints is accomplished by the muscles surrounding it as well as the extra-capsular and intra-articular

ligaments. These are discussed in detail in the following sections.

Knee Ligaments

Four major ligaments in the knee help it achieve complex kinematic motions as well as pull the knee together are the Anterior Cruciate Ligament (ACL), Posterior Cruciate Ligament (PCL), Medial Collateral Ligament (MCL) and the Lateral Collateral Ligament (LCL).

The intra-articular ligaments consist of the cruciate ligaments and the menisci. The cruciate ligaments are attached between the tibial plateau and the intercondylar spaces of the femur. The ACL is attached between the anterior tibial plateau and its primary function is to prevent the knee from anterior tibial translation and internal tibial rotation. The PCL is attached between the posterior tibial plateau and the medial formal condyle and it facilitates prevention of posterior tibial translation while hyper flexion of the knee and external tibial rotation. The menisci are crescent shaped fibrocartilage structures that are located on the articular surface of the tibia. They absorb the shock to the joint during motion and provide a restraint on the tibia from translation.

The MCL and PCL enclose the knee joint on the medial and lateral side respectively. The MCL extends between the medial epicondyle of the femur and the proximal end of tibia. The LCL runs between the femur and the proximal fibula. They primarily support the knee in adduction and abduction motions in the frontal plane.

Figure 2.2 shows the anterior, posterior and duperior view of the knee, detailing the bones, menisci and the major ligaments in the knee.

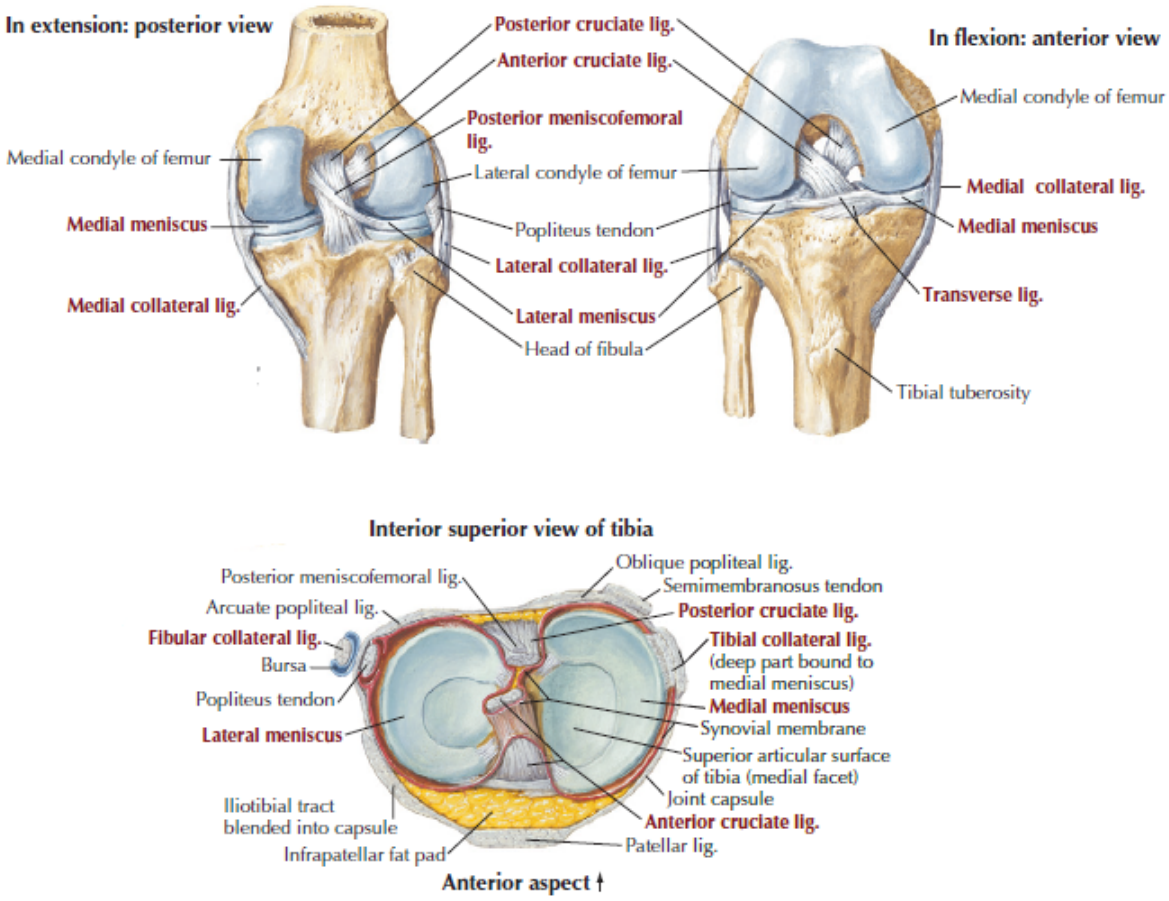

Figure 2.2: Anterior and posterior view of the knee (top) and superior view of the knee (bottom) (Adapted from Hansen (2022))

Knee Musculature

The major muscle groups that surround the knee are the quadriceps, hamstrings and gastrocnemius, as shown in Figure 2.3. The quadriceps comprise of the rectus femoris, vastus lateralis, vastus medialis and vastus intermedius which are primarily responsible for extension of the knee joint. The hamstring muscle group lying in the posterior thigh consists of the semitendinosus, semimembranosus and both biceps femoris long and short head muscles. Their primary function is assist flexion in the knee in activities like running,

gait and climbing stairs. The gastrocnemius muscles comprise of gastrocnemius lateralisis and gastrocnemius medialisis which also help in knee flexion and plantar-flexion.

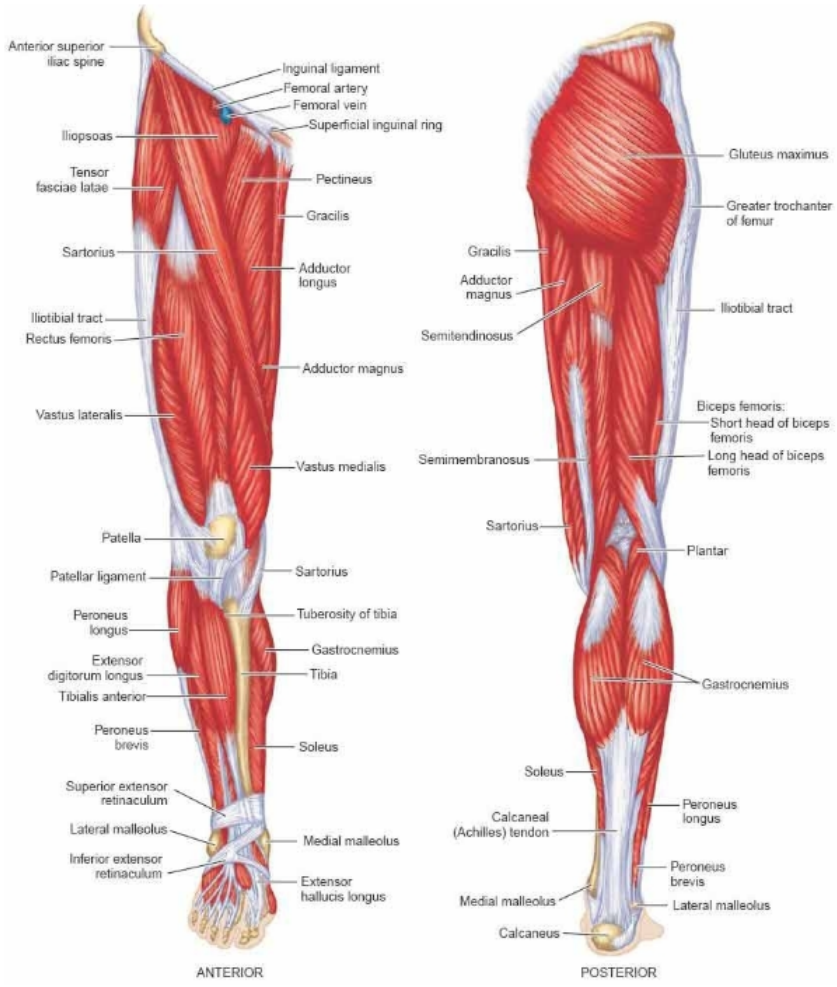

Figure 2.3: Lower limb musculature (Adapted from Hangalur (2014))

2.1.3 Anterior Cruciate ligament

Anterior Cruciate Ligament is made of dense collagen fibers structured like a band. It is reinforced by a ground substance and water making a composite matrix that also contribute

to the viscoelastic property of the ligament and act as shock absorbers (Chandrashekar et al. (2005)).

The ACL attaches between the anterior intercondylar region of the tibia and the lateral epicondylar region of the femur. It is made of two major fiber bundles called the antero-medial (AM) and posterolateral (PL) bundle, shown in Figure 2.4. The knee in extension causes the AM bundle to lax and the PM bundle to tighten. Whereas in flexion, the AM bundle tightens and the PM bundle goes lax. The PM bundle restricts the tibial rotation and stabilizes the knee during extension and the AM bundle restrains the anterior tibial translation (Petersen and Zantop (2007)).

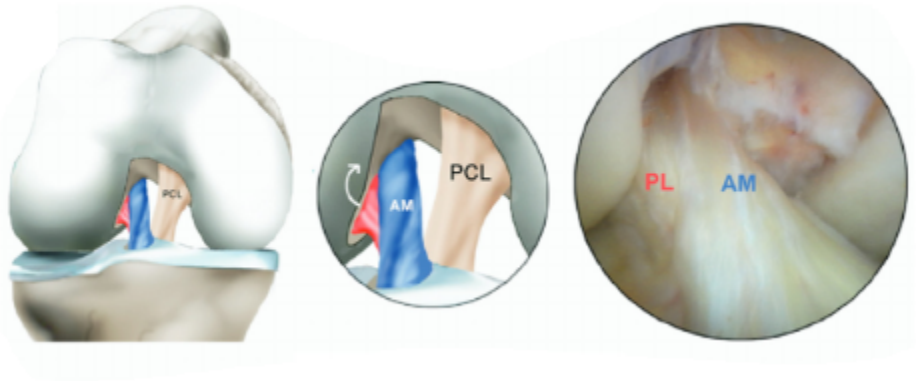

Figure 2.4: AM and PM bundles of ACL (Adapted from Sonnery-Cottet and Colombet (2016))

It is important in maintaining the stability of the knee. Any injury to the ligament due to its elongation or rupture can cause unrestricted motion of the femur further causing degenerative diseases in the knee.

ACL Injuries

As discussed in the previous section, ACL primarily provides restraint to anterior tibial translation and also provides stability during tibial rotation (Hangalur (2014), Yu et al. (2000)). Injury to the ACl can not only disrupt the functioning of the knee but it is also poses a risk of developing Osteoarthritis in future (Alexander Mitrichev and Wilson). In cutting and pivoting sports, the ACL injuries are the most frequent accounting for 64% of the knee injuries (Krosshaug et al. (2006)). The three main injury mechanisms identified by (Raines et al. (2017)) are direct contact, indirect contact and non-contact. A direct

contact injury is described as an external force applied directly at the knee. An indirect contact injury occurs when a body part other than the knee is impacted with an external force causing an ACL injury. The non-contact mechanism accounts for 60-70% of the injuries which occur due to a sudden change in direction of the leg or when its deceleration is coupled with ill-timed muscular forces causing the maximum load to be taken by the ACL, resulting in its rupture or injury. Cutting and planting and jump landing movements also widely cause injuries to the ACL.

Intrinsic and extrinsic factors contributing to the ACL injuries have been studies widely in the past. Intrinsic properties include the tibial properties, size of the femoral notch, characteristics of the ACL, Q-angle, Intercondylar width and alpha angle (Alexander Mitrichev and Wilson). The extrinsic factors include the activities being carried out and the biomechanical factors that are inherent to them while executing them. Control of the intrinsic factors to mitigate the injuries more difficult compared to the extrinsic factors. Use of knee braces has been applied as means to mitigate to the injuries to the ACL by providing a mechanical restraint to the knee. Knee braces have been employed to stabilize the knee joint and also provide support to ACL injured or deficient knees while rehabilitation. Although there is no common consensus on the outcomes of application of knee braces and the effectiveness of knee braces in providing knee stabilization is unknown.

2.2 Knee Bracing Effectiveness Studies

The primary reasons for the design of the knee braces have been to prevent injury in the ligaments or to restore the kinematics of the knee after a ligament injury. They stabilize the mechanics of the knee by restricting the translation of the tibia and its rotation in various anatomical planes under static or dynamic loading. One of the first studies conducted by Anderson et al. (1979) declared that the Anderson Knee Stabler helped in preventing ligament injuries and also predicted that the brace would help in reduction of tibial translation and valgus load to the knee. Although, the claims were not supported by sufficient proof of efficacy, this study lead to an increased popularity of knee braces. Numerous studies ensued to quantify the effectiveness of knee braces (Najibi and Albright (2005)).

2.2.1 Experimental Studies

Experimental research has been conducted to evaluate the effectiveness of prophylactic knee braces in reducing the risk of injuries in the knee ligaments and functional and rehabilitative

knee braces in providing support and protection to injured or repaired knee (Hewlett and Kenney (2019)). In-vivo methods such as motion capture analysis, EMG data acquisition and use of strain gauges at the knee while wearing a knee brace have been employed. In-vitro studies with the use of cadavers and surrogate knees have also been performed to quantify knee stability and risk of injury to knee ligaments.

In-Vivo Studies

Researchers have employed several in-vivo techniques to understand the efficacy of knee braces. Approach of direct measurement of ligament strains by invasive instrumentation of human participants with measurement devices is unethical. Hence, researchers have employed techniques of motion capture and Ground Reaction Force (GRF) measurement to derive the leg muscle forces, joint kinetics and kinematics, and knee ligament strains from reflective marker trajectories. Electromyography (EMG) measurement has also been used to monitor muscle activity and correlate it with brace effectiveness. The following section describes a few studies conducted using motion capture and EMG data collection to evaluate knee braces.

Ramsey et al. (2003) used videotaping method on four ACL deficient subjects for measurement of kinematics of femur and tibia by inserting Hoffman bone pins on the bones with reflective markers. EMG data was simultaneously collected for bicep femoris and rectus femoris activity while performing the activity of gait motion. Activity in semitendinosus decreased by 17% prior to footstrike with the brace. Following the footstrike, activity in bicep femoris decreased by 44% and activity in rectus femoris increased by 21% between unbraced and braced conditions. They concluded that although knee braces did not increase mechanical knee stability, they enhance the proprioception which causes a change in muscle firing timings and amplitudes resulting in an increased knee stability.

Gait kinetics and kinematics were studied in people with lateral knee osteoarthritis and valgus malalignment after 12 ± 4 years of ACL reconstruction surgery by Hart et al. (2016). Nineteen patients were included in the study. Motion capture technique was applied to extract frontal, sagittal, and transverse plane, knee and hip angles and moments with and without a knee brace while walking. In the sagittal plane, an increase in peak knee flexion angle by 3.4° and peak adduction angle by 1.3° was recorded. Substantial increase in peak knee flexion, adduction and internal rotation moments were also observed. In the transverse plane, peak knee internal rotation decreased by 1.6°, suggesting altered kinematics and kinetics in the patients after ACLR.

In a similar study conducted by Schween et al. (2015), 18 participants with knee

osteoarthritis were videotaped using VICON V-MX motion capture system with retro-reflective marker clusters places at leg joints during gait motion, while wearing an elastic sleeve brace. Using inverse dynamics approach, they calculated a decrease in knee adduction angle by 1.5° and decrease in knee adduction moment by 10.1%. It was concluded that the knee abduction angle and moments reduced in most parts phases of stance. The brace is suggested as a potential remedy for progression of disease in people with medial knee osteoarthritis.

Based on studies by Jung et al. (2008) and Hwan Ahn et al. (2011), laxity of the posterior knee can be improved after PCL injury by providing an anterior force to counteract the posterior translation. LaPrade et al. (2015) studied the forces applied by a dynamic functional knee brace to the posterior proximal tibia. They employed three dimensional motion capture technique, as shown in Figure 2.5, to evaluate the kinetics at the knee joint of six adults while performing the motions of seated knee flexion, squatting and stair decent, with and without the knee braces. An increase in force (average 45N) applied by the brace with increasing flexion angle was noted and the force continued to increase with increase in the flexion angle. During staircase decent, average force increased by 78.7 $\pm$ 21.6 N. Similar trends were observed for squatting motion. It was concluded that the forces applied by the brace to the posterior of tibia increased with increase in flexion angle. Improvement of knee laxity after PCL injury remained unanswered.

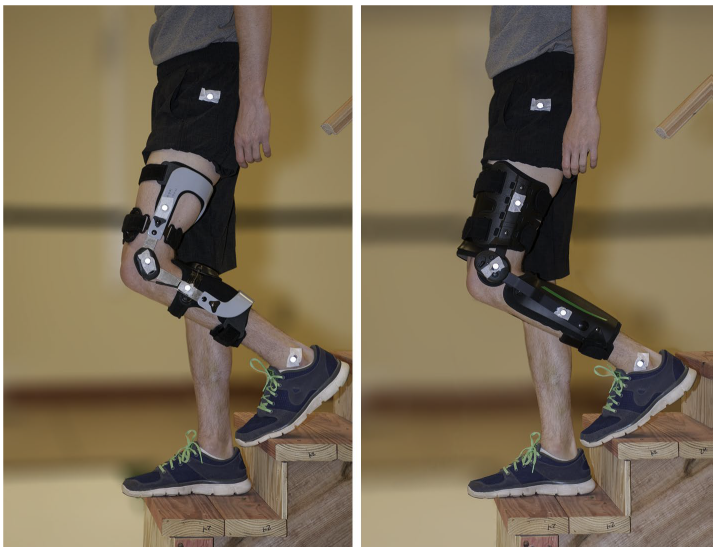

Figure 2.5: Motion capture while participant climbed down the stairs (Adapted from LaPrade et al. (2015))

In-Vitro Studies

In-vitro studies to quantify the effectiveness of knee braces in preventing ligaments injuries or providing protection after an injury often involves study of cadavers. Due to inherent difficulties of conducting research with cadavers and their inability to incorporate weight bearing, surrogate knee models have been developed by researchers to test knee braces.

Anterior Cruciate Ligament strain under the effect of six different prophylactic braces was evaluated by Paulos et al. (1991). A mechanical surrogate that was anatomically analogous to a human knee was constructed as shown in Figure 2.6. Femoral and tibial segments, functional hip joint mechanism, ankle and a torso were included. The ACL and MCL were modelled using Teflon coated, stainless steel cables that were couple with compression spring in series. Load cell were attached to the cables to evaluate the stresses. The surrogate was tested to closely mimic the human knee during dynamic loading. In order to place the brace over the limb, a coating of soft tissue that imitated the human limb in terms of compliance and curvature was planted over it. Impact test were then conducted for 0° and 30° flexion angle, with the ankle free to rotate and move vertically. A system of ramped and gravity accelerated impact trolley was setup to conduct these tests. They recorded the tension in ACL and MCL and the peak impact loads as a function of time were noted. Based on the tests, they concluded that the reduction in the mean MCL peak load was 21.95% $\pm$ 6.92% and in ACL it was 38.9% $\pm$ 15.32%. The decrease in peak force in ACL was greater that the decrease in the peak force in MCL. It was also noted that with the braces on, the impact duration was increased based on tension initiation time in the ligaments, suggesting a reduction in net impact momentum and thus protecting the ligaments from injury.

Baker et al. (1989) completed an in-vitro study with the use of a lower extremity cadaver with and without wearing prophylactic and functional braces to evaluate the change in abduction angle in the knee and the load in ACL and MCL while applying direct lateral loadings. The study was conducted in two steps. The first step involved applying static loading to create adduction and external rotation on the cadaver knee to simulate an upper body contact with a fixed foot. The second step involved simulating a clipping injury by applying a lateral impact load with a fixed foot and a suspended femur with a free knee (Figure 2.7). Force transducers were applied to the ACL and MCL, and femur and tibia were attached with an electrogoniometer with bone screws and Steinmann pins. The cadaver leg was set up such that the head of the femur was prevented from dislocation by fitting into a socket, which was free to move in the vertically. The femur was loaded with a constant vertical load and the quadriceps force applied to achieve a desired flexion

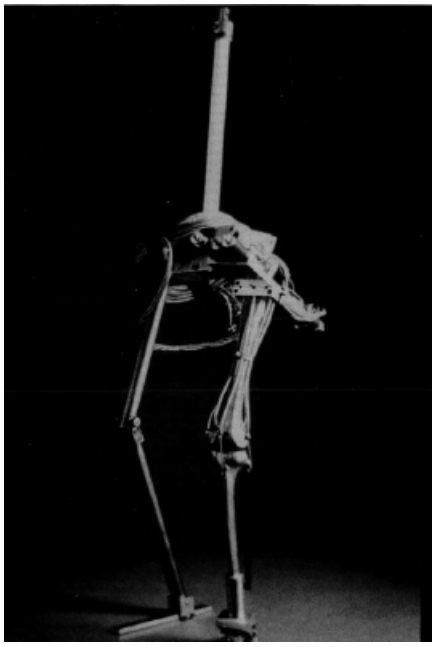

Figure 2.6: Surrogate leg tested in dynamic loading (Adapted from Paulos et al. (1991))

angle by balancing a weight using a pulley system. Internal femoral rotation was restricted using a clamped bar. The impact loading was applied by swinging a weight attached to a pendulum at a fixed angle. This test was conducted six times at knee flexion angles of 0° and 20° in lateral, posterior oblique and anterior oblique directions. Two sets of these tests were performed, one with MCL and intact and the other one with the MCL sectioned. They found out that the functional knee braces caused a reduction as high as 53% in knee abduction angle compared to prophylactic knee braces where the maximum decrease was 25%. Also, they recorded a higher reduction in abduction angle when the MCL was intact as opposed to when it was cut (as low as 3% in prophylactic braces). No clear trends could be concluded for the peak MCL force with the addition of brace. A greater reduction in peak ACL force was noted during flexion in functional braces when compared to prophylactic braces, with the MCL intact.

In another study by Meyer et al. (1989), two prophylactic braces were studied for their effectiveness. Three parameters considered to determine effectiveness were relative strain attenuation in MCL, gross stiffness exhibited by cadaver with and without the brace and the total failure load. Twenty fresh frozen cadavers with no history of musculoskeletal disease at the knee joint were tested. Two LMSG's were affixed to the MCL, one at the

Figure 2.7: Cadaver leg being hit by a pendulum load (Adapted from Baker et al. (1989))

posterior fibre bundle and the other at the longitudinal fibre bundle. A testing fixture, as shown in Figure 2.8, was designed such that the ankle was fixed at one end. The hip center was free for internal or external rotation and adduction or abduction. To simulate weight bearing, a pneumatic actuator at the hip applied a compression load axially at the knee. Dynamic valgus impact loading was applied by a steel impactor at a speed of 100mm/sec. Liquid Metal Strain Gages (LMSG) were used to monitor the strain in the MCL as measure to quantify performance of the brace. Peak sub-failure strains were reported to have reduced significantly ($p<0.005$) in braced configuration.

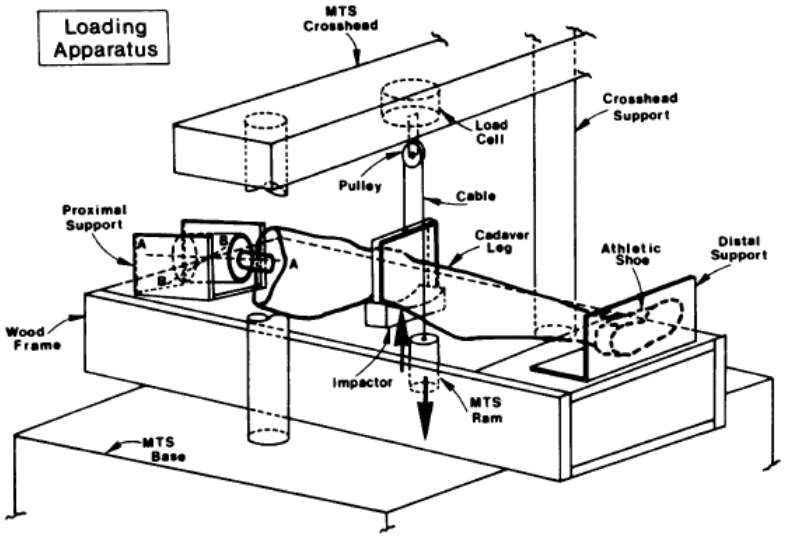

Figure 2.8: Testing Apparatus (Adapted from Meyer et al. (1989))

Erickson et al. (1993) used a surrogate-cadaver hybrid model to evaluate the ability of prophylactic knee braces in reduction of ACL and MCL strains under dynamic valgus impact loading. Eight cadavers were tested with four different prophylactic knee braces and tested at 0 and 30 flexion angle, while an impact load was applied laterally using a custom developed apparatus shown in Figure 2.9. Hall Effect Strain Transducers were instrumented at both ACL and MCL to measure the strains. They concluded that the impact force significantly reduced at impact point, but the reduction in ACL elongation was not significant.

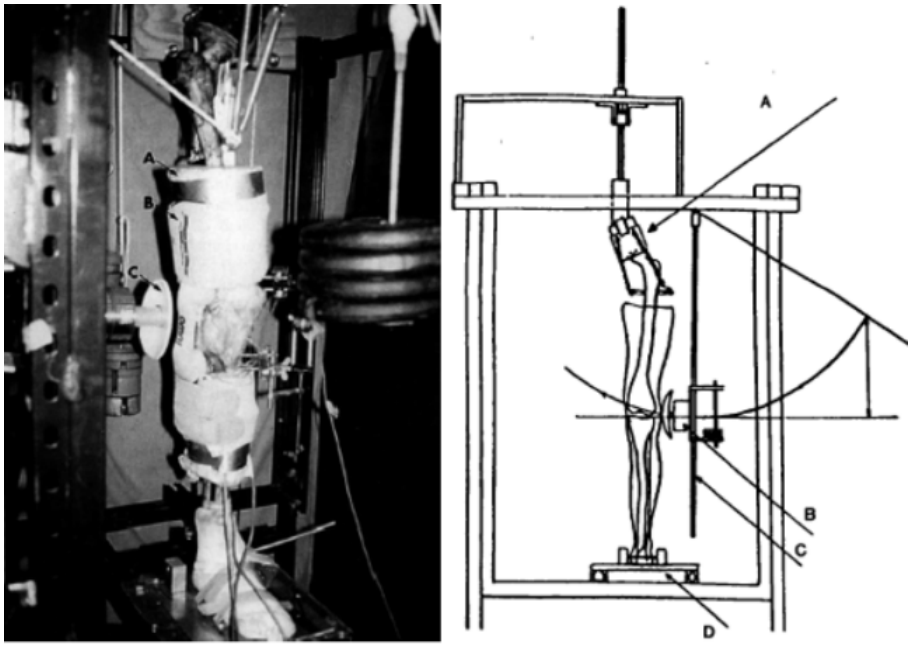

Figure 2.9: Apparatus to test hybrid Surrogate-cadaver model (Adapted from Erickson et al. (1993))

2.2.2 Computational Models in Knee Bracing

Haris and Beng Chye Tan (2021) developed a computational model to assess the effectiveness of a single-hinged knee brace in treatment of a knee with osteoarthritis. An optimal solution for the tightening of the elastic strap, torsion spring stiffness and brace pre-tension was implemented to achieve reduction in stresses in the femoral cartilage and tibial cartilage at varied flexion angles. A subject specific knee model consisting of the femoral and tibial cartilages and menisci was developed to simulate the knee brace. A strap-muscle system was developed to extract stiffness in axial, tangential and radial directions to input for the torsional spring of the knee brace. They noted that the equivalent stiffness were increased with the increasing strap tightness. At higher flexion angles, torsional spring provided an aid in reducing stresses, while the brace pre-tension provided an aid at low flexion angles. They concluded that use of a hybrid model would help minimize the stresses over the complete flexion range.

In a study by Pierrat et al. (2015a) to evaluate a hybrid hinge-elastic knee brace and its effectiveness in reducing drawer, numerical analysis was done. A subject-specific model

was developed by segmenting a CT scan of a leg. Skin made of shell elements was added on the model. The brace was modelled consisting of three separate regions: the fabric of the brace, straps and rigid links. The orthoses was modelled using quadrilateral, linear elastic shell elements and the hinge joint between the rigid links was modelled using connectors with a stop feature to prevent hyperextension (Abaqus 2010). To model the contact between the skin-orthoses and skin-knee soft tissues, coulomb friction model was used. The analysis was carried out in multiple step. In the first step, a pre-stress to the skin was applied and a displacement was applied to the orthoses to fit to the joint. In the second step, this displacement was released to compress the joint and leg. The straps were pre-stressed in this step. The last step involved applying a posterior-anterior drawer to the tibia while keeping the femur and patella fixed. To quantify the mechanical stability, effective stiffness and pressure applied to skin were measured to apply the technique of parameter optimization to identify the key factors affecting brace design.

In a following study by Pierrat et al. (2014), FE knee model of a generic knee brace was developed and validated with an experimental testing machine. This was further used to evaluate the influence of different design parameters on kinematics of the knee. A test machine was used to test a surrogate limb under three quasi-static kinematic loading conditions: flexion, varus rotation and anterior tibial translation. The machine was instrumented to measure the reaction forces and moments at each axis. Once this FE model of generic knee brace was validated, two functional and two rehabilitative orthoses were investigated for their ability to prevent laxity and instability. The design parameters tested were the effect of strap tightening, length of brace and the size of brace. Indicators of performance were the slopes of load-displacement curves for the above three kinematic loading conditions, indicating the effective stiffness at the knee joint.

2.3 Cable stabilized brace inspired by Stoko

The cable stabilized knee brace uses a system of pre-tensioned cables to provide mechanical stability to the knee. This cabling system runs through a compression tight, along designed pathways, to provide compressive forces in localised regions of the leg such that it brings the knee back to its natural configuration, as shown in Figure 2.10. When the knee moves out of alignment, the non-extensible cables are pulled into tension similar to the ligaments, to stabilize the knee mechanics. The tension in the cabling system can be varied by the user using a dial system attached at the upper back of the tight. One end of the cable was fixed at the waistband of the tight. The dials when rotated, wrap the other end of the cables around them, pulling and locking them into tension.

2.3.1 Stabilization Mechanics

In the kinematic conditions of valgus, an abduction moment acts on the knee causing an increased loading on the MCL. The increased stress causes an increase in ligament strain, which when exceeds a threshold makes the ligament prone to injuries. The cabling system in the brace is designed such that it pushes on the anchor points at the hip and the calf, and pulls at the MCL, causing an adduction moment about the knee. The resultant is a reduced effective moment at the knee, decreasing the strain in the ligament. In a similar manner, it provides support to LCL during varus motion.

The tensioned cables crossing through the shin and the calf muscles apply forces to restrain the translation of tibia. The cables at the anterior of tibia provide forces to the posterior direction, stabilizing the anterior tibial translation, helping reduce the strain at the ACL and meniscus. Similarly, support is provided during posterior tibial translation, preventing injuries in PCL and meniscus.

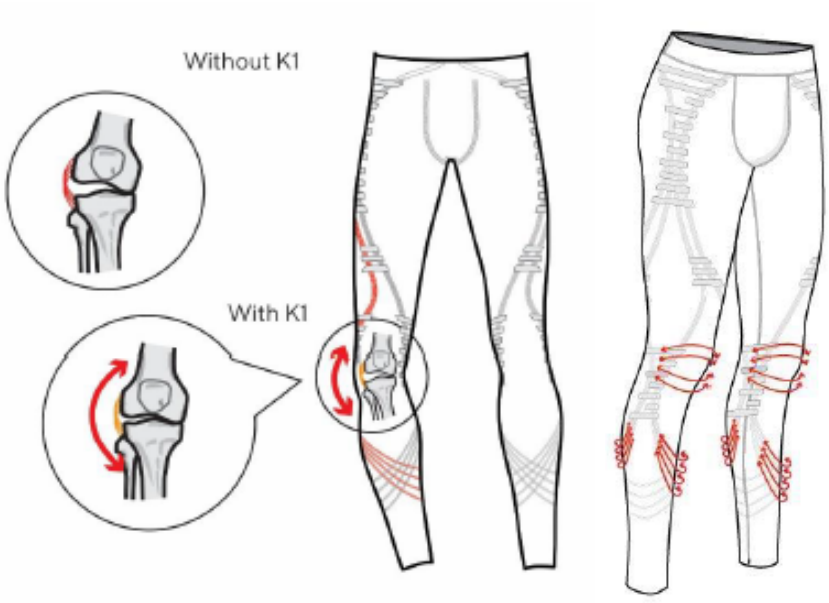

Figure 2.10: Mechanical stabilization provided by the knee brace (Adapted from Stoko (2015))

Along with the cabling system, the compression tight is also theorized to increase knee stability and recovery due to improved proprioception, reduce fatigue and increase the blood flow.

2.4 Precursor Studies

An overview of the development of the Finite Element model of the knee is given in the following section. It is crucial in understanding the further development of the knee brace FE model, its validation in quasi-static loading and the jump landing simulations of the knee conducted in the braced configuration.

2.4.1 Finite Element Model of the Knee

A Finite Element model of a knee (shown in Figure 2.11) was developed by Rao (2020). The kinematic responses of the model were verified by comparing them to published data. Single-leg jump landing simulations conducted by Bakker (2014) were then replicated on this model to measure the strain in ACL and compared to the results of in-vitro experiments conducted by Bakker (2014) and Polak (2019).

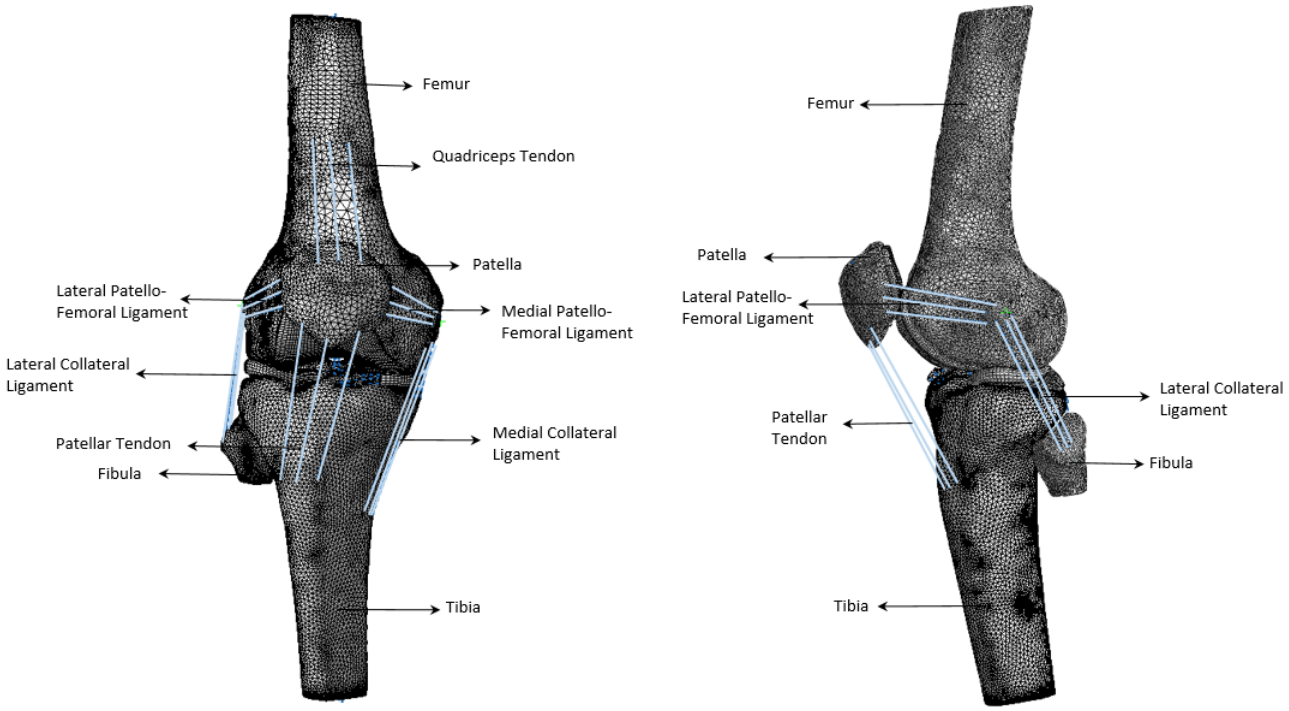

Figure 2.11: Front view of the developed FE model of the knee

The process of development of the model started by imaging a cadaver specimen of a 50th percentile male. MRI and CT scans of the cadaver were collected. Images of the knee in sagittal, transverse and frontal plane were taken. These images when stacked on each other in all three planes, output a solid geometry of the knee. 3D geometries of bones, meniscus and cartilages were identified and extracted from the consolidated image slices in a software called 3D Slicer, using a combination of manual and automatic segmentation processes as in Figure 2.12. These extracted geometries were then imported to SolidWorks for further smoothing and post-processing.

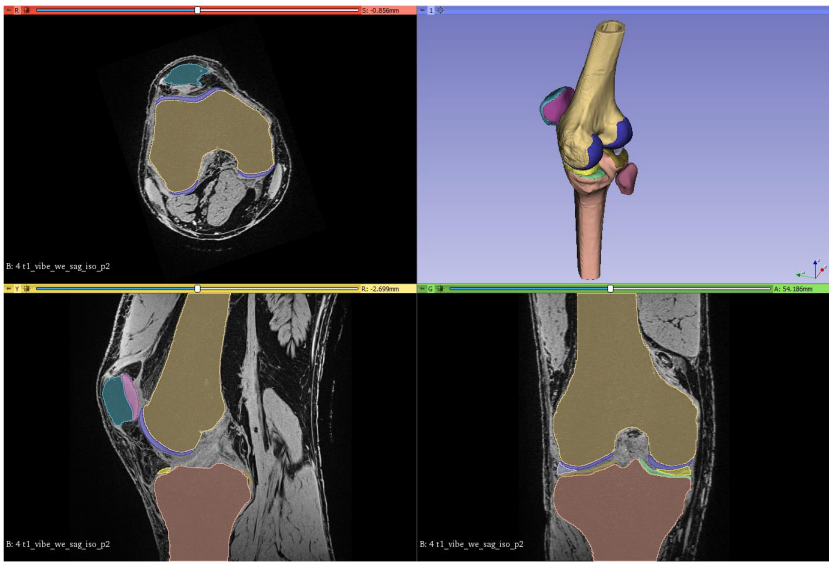

Figure 2.12: Knee segmentation from MRI scans (Adapted from Rao (2020))

Attachment sites of all ligaments were identified on the cadaver using a process of digitization to be replicated on the FE model. Internal surfaces of the bones were exposed and the identified bony landmarks were referenced as the attachment sites of ligaments. A coordinate measuring device was used to record the locations of ACL, PCL, MCL and LCL attachment sites. Coordinates of these locations were matched to the 3D model in 3D Slicer and later imported to Abaqus CAE. The overview of the process is given in the Figure 2.13.

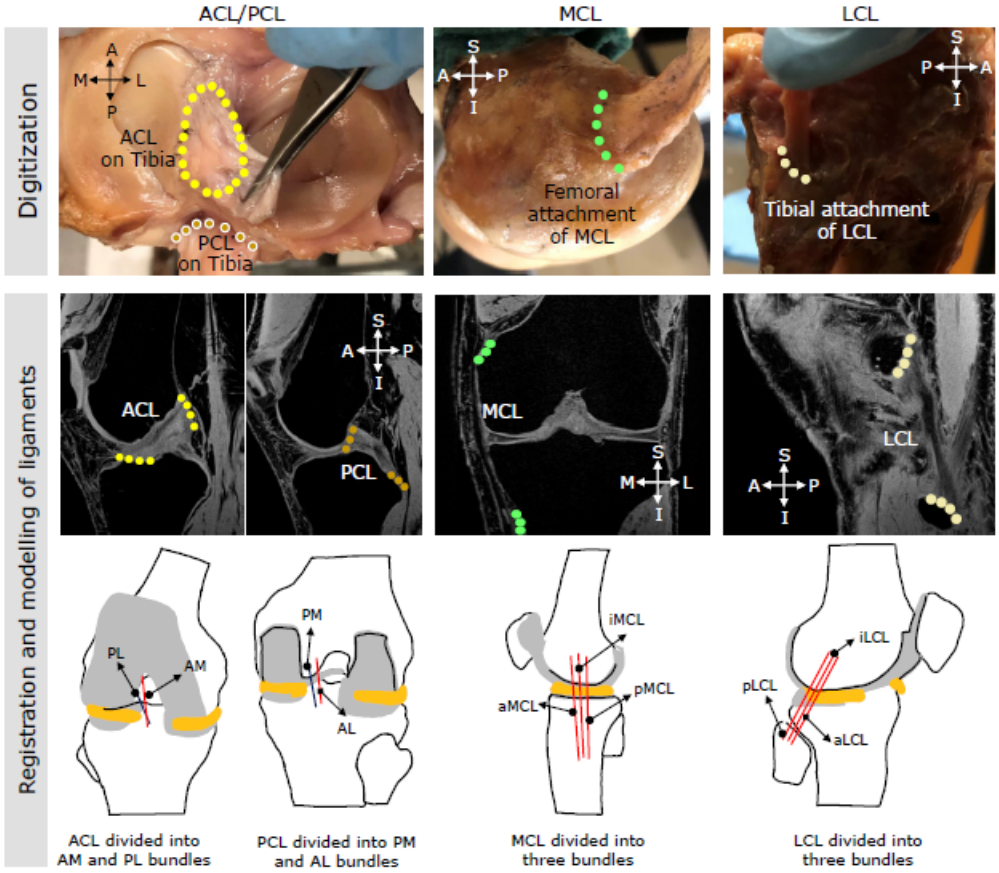

Figure 2.13: Ligament attachment on FE model from digitization process (Adapted from Rao (2020))

Bones were modelled with stiffer material properties, hence they were meshed using tetrahedral elements in Hypermesh. They were assigned as rigid bodies in the FE model. The meniscus and cartilages were softer tissues with lower material stiffness, hence they were modelled using hexahedral mesh elements in a software called IA-FEMesh. These meshed geometries were then imported to Abaqus and assembled. The cartilages were constrained to their respective bones using TIE constraint such that no relative motion was allowed between them. A frictionless contact was given between the cartilages and meniscus for smooth sliding. Table 2.4.1 shows a list of material properties assigned to these components.

Anatomical Structure	Definition in Abaqus	Young's Modulus (MPa)	Poisson's Ratio	Reference Study
Femur Tibia Patella Fibula	Rigid	8000	0.3	Haut Donahue et al. (2002)
Femoral Cartilage Lateral Tibial Cartilage Medial Tibial Cartilage	Deformable	20	0.45	Akizuki et al. (1986)
Lateral Meniscus Medial Meniscus	Deformable	59	0.49	LeRoux and Setton (2002)

Table 2.1: Material properties assigned to anatomical structures (Adapted from Rao (2020))

For the modelling of ligaments, axial connector elements were used and non-linear force versus displacement curves were assigned. The ACL was modelled as two connectors, representing the anteromedial and posterolateral bundles. Force versus displacement data from Chandrashekar et al. (2005) was used for the stiffness of the ACL. Stiffness parameters for all other ligaments were replicated from Blankevoort et al. (1991). A list of stiffnesses of the major ligaments is given in the Table 2.4.1 is given below.

Ligament	Ligament Bundle	Stiffness parameter, k	Strain at extension, ϵ	Reference Study
ACL	Anteriomedial Posterolateral	NA	0.06 0.10	Chandrashekar et al. (2005) Blankevoort et al. (1991)
PCL	Anteriomedial Posterolateral	9000 9000	-0.15 -0.03	Blankevoort and Huiskes (1996)
Superficial MCL	Anterior Middle Posterior	2750 2750 2750	0.04 0.04 0.03	Blankevoort et al. (1991)
LCL	Anterior Middle Posterior	2000 2000 2000	-0.25 -0.05 0.08	Blankevoort et al. (1991)

Table 2.2: Material properties assigned to ligaments (Adapted from Rao (2020))

The kinematics of the model were verified for flexion, abduction, internal rotation, anterior drawer and Lachman test. Jump landings simulations were then conducted by inputting the dynamic kinetic and kinematic boundary conditions from Bakker (2014) for ten participants. Comparisons for ACL strain and meniscus strain were made between the computational and experimental data to validate the FE model of the knee.

The FE model of the knee brace in the current study was developed on this validated FE model of the knee. The results from single-leg jump landing simulations were also used in the current study for comparison with the simulations run with the knee brace on.

Chapter 3

Methodology

3.1 Overview of Experimental Analysis of the Knee Brace

To evaluate the effectiveness of the knee brace, experiments were conducted by the Research and Development Team at Stoko. The knee brace was tested using a custom designed Knee Testing Fixture (KTF) and a surrogate leg model (Figure 3.1), both of which were developed in-house. The results from the FE model of the knee brace developed in the current study were later compared to the available experimental data.

3.1.1 Design of Knee Testing Fixture

The surrogate leg was developed by casting rubber, implanted with an anatomically accurate model of the knee. The KTF has four degrees of freedom and a rigid testing frame onto which the mechanisms designed to achieve motion are mounted. The KTF was developed to operate motion along each axis independently. This gives it the capability to achieve isolated motion along each axis and also perform complex motions to simulate injury mechanisms. The four axes of motion are varus/valgus arm, flexion/extension arm, tibial internal/external rotation and anterior/posterior drawer. Each of these axes are actuated by respective stepper motors and instrumented with load/torque cells to measure the load/moment at the knee. The tension in the cables of the brace is measured using a spring scale.

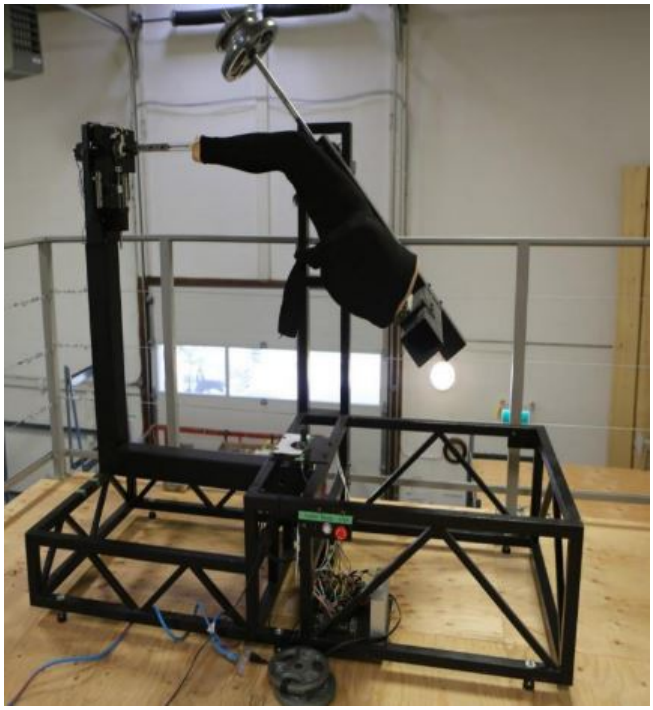

Figure 3.1: Knee Testing Fixture and the surrogate leg with the Stoko K1 knee brace

3.1.2 Test Methodology

For the validation of the current FE model of the knee brace, experimental tests for varus and valgus loadings conditions were used. The knee brace was put on the surrogate leg and tension in the cabling system was varied to desired values. The load cell was calibrated for the moment about the knee. Feedback for angular displacement about the varus/valgus axis at the knee was returned. The end at the hip of the leg was fixed. The ankle was free to translate along the axis of tibia and rotate internally or externally about this axis.

The test was conducted in the following sequence of steps:

- The leg was positioned at the zero position.
- Tension in the cabling system was set to a pre-determined value.
- An initial 20^o flexion angle at the knee was achieved by actuation.
- Quasi-static angular displacement of 0^o through 9^o was applied for varus/valgus.
- The leg was returned to the initial zero position.

This sequence was carried out for both varus and valgus motions. Repetitions were done for three primarily strategized cable pre-tension values. Feedback for the measurement of displacement was output throughout the motion and the moment at the knee was recorded from the load cell.

After processing this returned data, load-displacement curves for each motion at every pre-tension value of cabling system were created. These curves were compared against the baseline load-displacement curve at 0N pretension. Load reductions at the final position of the motion were calculated for each pretension value to evaluate the effectiveness of the knee brace.

It was hypothesised that with the increase in cable pre-tension, the load reduction at the knee would also increase. A higher load reduction would imply a decreased loading experienced by the ligaments in the knee, thus decreasing the chances of injury to them.

3.1.3 Measurement of the Leg Stiffness using Indenter

The compressive stiffness of the surrogate leg was measured using a custom developed indenter. An external piston cap was assembled to the indenter such that the internal piston could move through the hole in the piston cap. In order to collect data for stiffness calculation, the leg was placed while restricting the motion of the limb by applying an external force on it. The indenter was then placed on the desired region of the leg and force was applied manually to move the inner piston to a pre-determined displacement, while applied load was simultaneously noted. Repetitions were made to collect force data for varying displacements. Force versus displacement data for inner thigh, middle thigh and outer thigh regions of the leg was collected.

3.2 Development of Finite Element Knee Brace Model

The FE model of the knee brace was built on an existing FE model of the knee developed by Rao (2020). Figure 3.2 shows a flowchart of development of the FE model of knee brace.

3.2.1 Modelling of External Leg

FE model of an external human leg was built on the existing FE knee model previously developed by Rao (2020). Similar to Hangalur (2014) and Erickson et al. (1993), the

Figure 3.2: Overview of the work flow to assess the knee brace

external leg was built such that it encompassed the knee and provided an interface for mounting the knee brace. The contribution of the leg to the knee or the knee brace mechanics was not critical. However, its creation allowed for the cable tubes to be attached to it and the cables to smoothly slide on it. The following section describes the steps followed to model it.

Creation of Solid Leg Model

An existing open source model of the human leg was used. The model was a "Standard Triangle Language" model which described a triangulated surface mesh of the leg. Processing was done on this model to extract a 3D solid model. An overview of the processing steps is shown in Figure 3.3.

The triangulated surface mesh model was coarse and jagged. For smoothing, it was imported to a 3D meshing software called MeshLab, where duplicate vertices and surfaces of the triangles were removed. Laplacian Smoothing of the mesh was performed next. This feature adjusts the nodal location of each of the vertices based on their average position from adjacent vertices to improve the overall quality of the mesh. Point cloud of the smoothed surface mesh was exported.

The point cloud was then imported to SolidWorks (Dassault Systemes, Waltham, MA, USA). Using the Surface Wizard functions, the density of the points was reduced and made uniform in order to remove outlier points to obtain a further smoothed surface. Next, a

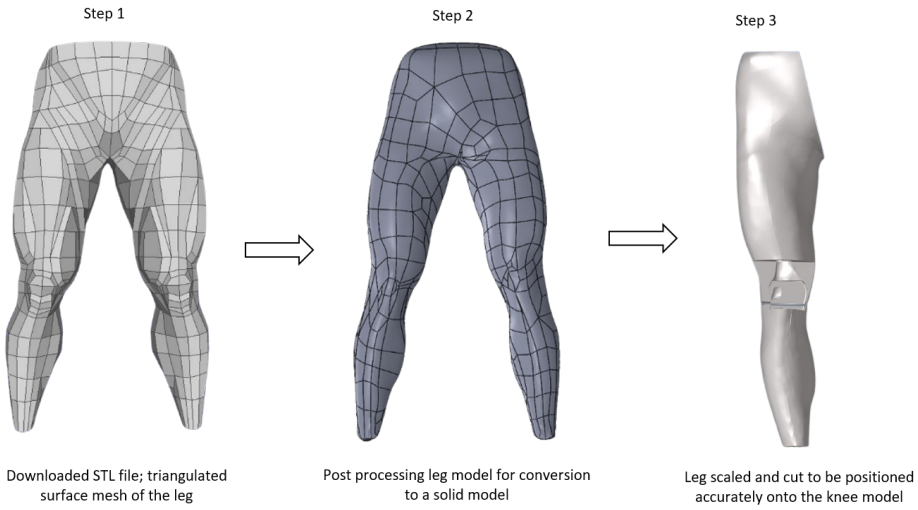

Figure 3.3: An overview of processing of triangulated surface mesh to a meshed leg

continuous and closed surface was wrapped around the point cloud. Creation of the closed surface allowed for its conversion to a solid body in SolidWorks.

The solid geometry of the leg was imported to Abaqus. To position the leg on the 3D knee model, MRI scans which were used by Rao (2020) to extract the 3D knee model were referenced. The leg was scaled to the size of the leg in the MRI images. The position of the leg on the knee was not required to be accurate hence the solid leg was manually translated and its position on the knee was approximated by referencing the cut section views of the model with the MRI images (Figure 3.4).

Once the leg was positioned, the tibia and femur bones in the knee model were subtracted from the leg to create a cavity for placing them. Geometry towards the front of the leg was cut to expose the patella, menisci and cartilage as shown in Figure 3.5. This was done to prevent the leg from making contact with the patella and inhibiting its motion to unnaturally modify the kinematics of the knee joint. A partition in the leg was also created in the medio-lateral plane along the knee joint (Figure 3.5) to accommodate for motions of flexion and extension.

Meshing

The leg material had a stiffness higher compared to the load bearing members of the knee joint and the stress gradient was low. It was also partitioned at the knee joint line

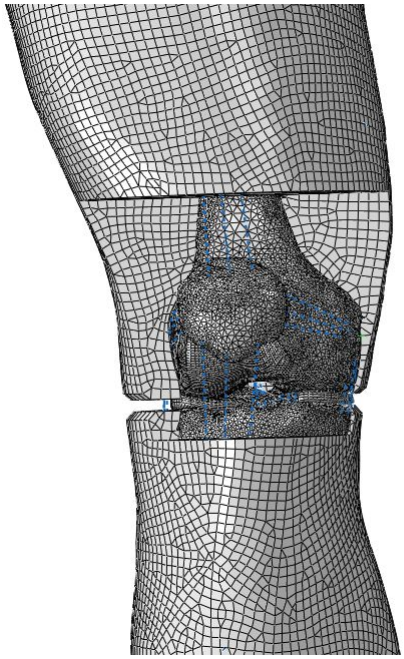

Figure 3.4: Front view of leg placement on the knee

making its contribution to effective stiffness of the knee joint non-critical. Therefore, a tetrahedral mesh was assigned to the leg. To maintain the geometrical curvature of the surface and a more accurate measurement of contact stresses (due to cabling system) at the surface, a quadrilateral dominant mesh was assigned to the surface.

The extracted geometry of the leg from Abaqus was meshed in HyperMesh (Altair Engineering, Inc., Troy MI, USA) as shown in Figure 3.6. First, the surface of the leg was meshed with a 4-node quadrilateral dominated mesh using feature. A quality check was conducted on the generated mesh for warpage, aspect ratio, minimum length and maximum length using feature. The mesh elements that did not pass the quality criterion were corrected manually. Next, a 4-node solid tetrahedral mesh, enclosed by the created surface mesh, was generated using the Automesh feature in HyperMesh. The interface between the quadrilateral mesh and tetrahedral mesh was given using 5-node pyramid mesh.

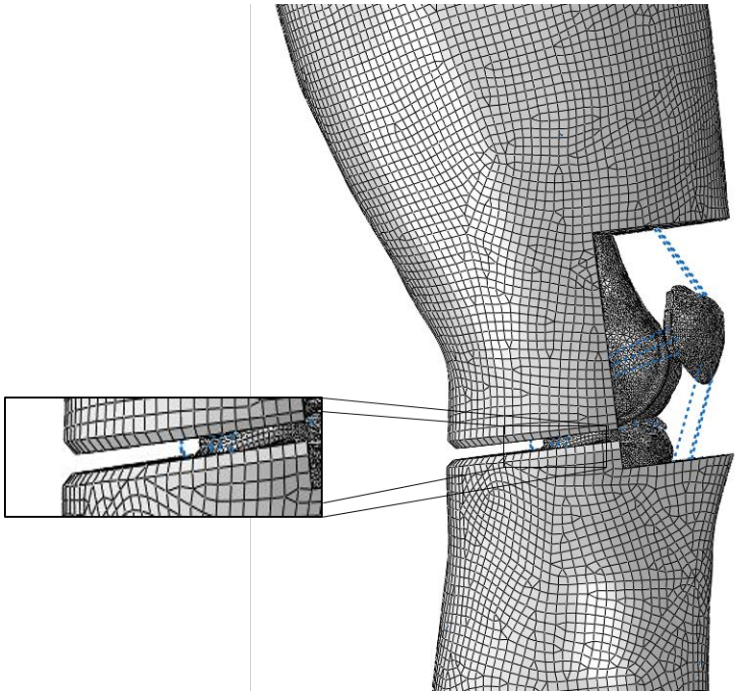

Figure 3.5: Partition of the leg at the knee

3.2.2 Modelling of Cabling System

The knee brace consists of eight cables running parallel, which then diverge into two sets of four cables each. The cabling system in the model constitutes of the cables and their corresponding cable tubes. The support to the knee was theorized to be primarily from the forces from equivalent cable pre-tension. This allowed for each set of four cables to be modelled as a single cable in the FE model. Therefore, the pre-tension later applied to the cables was four times the pre-tension measured experimentally in individual cable.

Modelling the Tension Cables

The cables in the cabling system were modelled as spline wires in Abaqus CAE. The spline was created by visually approximating the cable pathways on the leg. The reason for this was that the knee brace conforms to the shape of the leg, consequently changing the pathways of the cable relative to the knee depending on the participant wearing it. Moreover, cable pathways relative to the knee also vary every time a participant wears it,

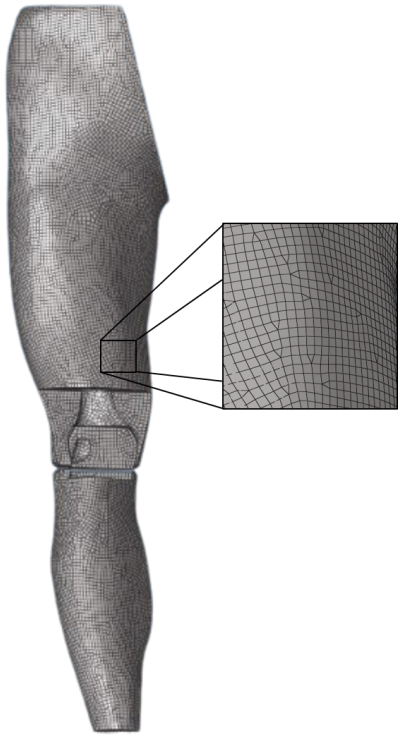

Figure 3.6: External leg meshed in HyperMesh

further justifying the approach.

To create the cable geometries, nodes of the meshed surface of the leg that lay in the pathway of the cables were recorded. Coordinates of these recorded nodes were extracted and connected in sequence to create cubic spline wires in the shape of the cables.

Modelling the Cable Tubes

Tubes were modelled to replicate the pathways through which the cables run in the knee tight. The contact between the cables and these tubes constrains the cables, allowing them to slide on the leg only along the axial direction. Detailed reasoning for their modelling is discussed in Section 3.2.3. The coordinates that were previously extracted for creation of the cables were imported to SolidWorks. A spline was created by connecting these points. At one end of the spline, a plane was created perpendicular to the curvature of the spline. On this plane, a hollow circular cross-section of the tube was sketched. This sketch was

then extruded along the axial direction of the spline to create a tube. This process was followed for creation of both the tubes of the modelled cabling system.

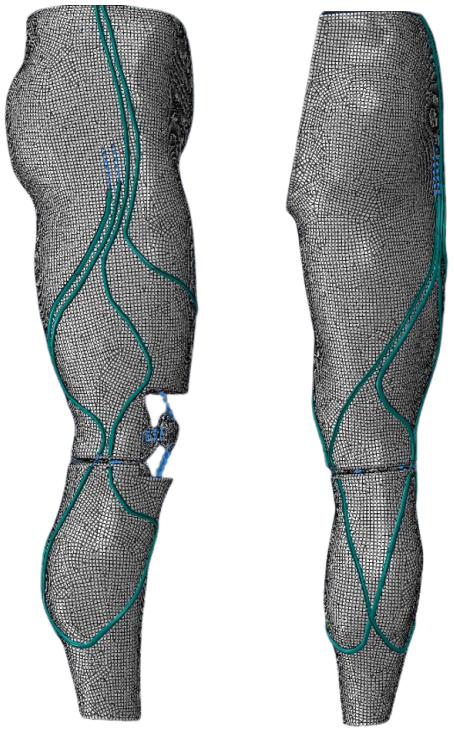

Figure 3.7: Side and back view of the cabling system on the leg

Meshing

The cables and the cable tubes were meshed in Abaqus CAE. The cables were meshed with 2-node truss elements. Because the wire geometry of both the cables was one dimensional, the mesh was automatically generated.

The cable tubes were meshed with 8-node hexahedral mesh. Because of the non-linear geometry of the tube, it was not possible to automatically generate the mesh. Therefore, the tube was partitioned into multiple smaller cells. Technique of sweep meshing was then applied to generate the mesh. This technique creates a surface mesh at the specified face or edge of the geometry and then sweeps that mesh along a sweep path.

First, at cross-sections at the ends of each of the cells, the number and placement of element nodes were specified at the circular edges. This method is called edge seeding.

Edge seeding was also applied at the edges along which the mesh was swept. Next, a quadrilateral mesh was created at the seeded faces of the cells. This mesh was then swept along the sweep path along the length of the cell to create a solid hexahedral mesh. This process was repeated to mesh all constituent cells of both the tubes.

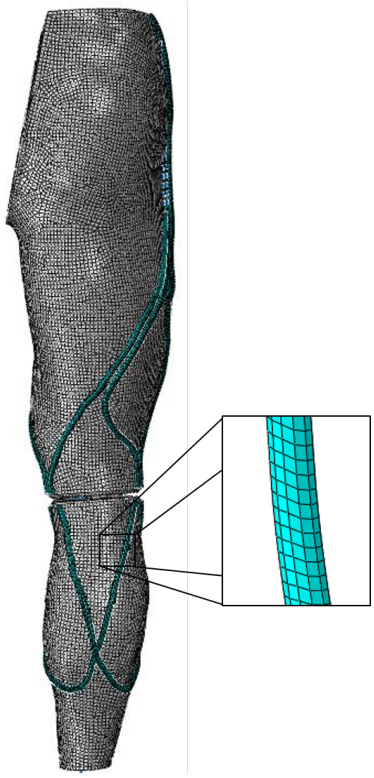

Figure 3.8: Meshed cable tubes

3.2.3 Finite Element Model Definition in Abaqus CAE

The meshed model of the external leg was imported to Abaqus CAE and assembled with the modelled cabling system. Suitable material properties and element types were assigned to the assembly components. Contact and constraints were defined to accurately model the interactions between these components. Modelling methods were employed to achieve uniform pre-tension force across the cables. The details of the model setup have been explained in detail in the following sections.

Element Assignment

The pretension cables were meshed using 2-node interpolation linear elements. They were assigned as T3D2 truss elements which are constant stress elements that support loading and deformation in the axial direction only. At their nodes, they are connected to the adjacent elements with a pin joint. This allowed the cables to conform to the designed cable pathway and the leg while sliding on it due to the knee kinematics.

The cable tubes in the cabling system were meshed with 8-node linearly interpolated hexahedral elements. C3D8R element type was assigned to them. A reduced integration element uses a lower order of integration for the calculation of stiffness matrix. This allowed the computational time to be reduced significantly.

One of the disadvantages of reduced integration is that it causes the elements to distort unnaturally because of a single integration point for calculation of its stresses and strains. This can cause the strain calculation at the integration point to be zero, leading to a distorted mesh resembling the shape of an hourglass. In order to prevent this phenomenon of hourglassing, an artificial strain energy was introduced to the elements. This hourglassing control is called hourglass stiffness, which was added to the elements in Abaqus.

Lastly, the external leg was meshed using 4-node linear interpolation tetrahedron elements and 5-node linear interpolation triangular prism elements at the surface. Hence, C3D4 and C3D5 stress elements from the element library were assigned to the mesh.

Cable Pre-Tension Modelling

The cables in Abaqus were assigned with truss elements. A feature to note about these elements is that no initial stiffness is offered by them in the directions perpendicular to their axis. Hence, if a loading is applied perpendicular to the centerline or no constraints are given in this direction, it results in non-convergence and numerical singularities while calculating its stiffness matrix. This dictated the pre-tension load application and contact formulation in the cables.

Several methods were identified to apply tension to the cables. An axial force could be applied while a translational constraint is applied to the truss elements in the normal direction. This required a coordinate system to be created such that one of the coordinate axes was in the direction normal to the elements and other coordinate axis in the axial direction of the cable. This approach was not suitable for the current model because the geometries of the cables were non-linear and application of boundary condition non-linearly in space was not possible in the software.

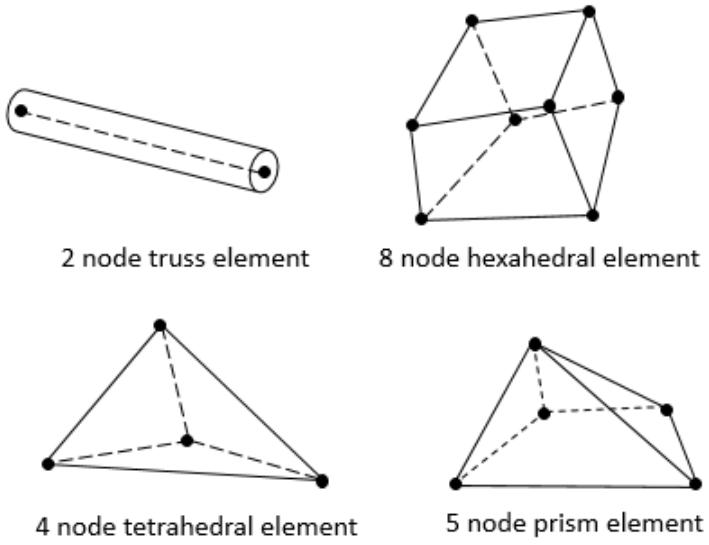

Figure 3.9: Elements assigned

Weak springs in the normal direction could also be applied to the truss elements to prevent the loss of stiffness in normal directions. Once an initial stiffness is achieved in the cables, the springs can be removed in subsequent steps. This method of applying weak springs to truss elements was not supported in the Explicit Dynamics module, making it an unsuitable approach.

Formulation of contact to the cable in the normal direction was another approach. Numerical non-convergence is seen in the first few increments. However, as soon as contact is made between the cable and the adjacent surface, the calculation of stiffness matrix achieves convergence. Therefore, a cable tube was modelled as the contact surface. It introduced a stiffness in the normal direction of the cable as well as constrained the cable to the designed pathway.

The tension was induced in the cable by applying a displacement to it. However, it had to be applied while the ends of the cable were fixed to the leg. To implement this, a small section of truss elements of the cable wire were replaced with axial connector elements. Axial connectors are a combination of springs and dampers to which can be modelled to output a linear or non-linear force versus displacement response. A displacement boundary condition was applied to this connector section, pushing the connector section into com-

pression and pulling the cable on either sides of the connector into tension. Figure 3.10 shows an example of its implementation. Because the cable geometry was non-linear and had some portions of relatively low radii of curvatures, multiple section of connectors were modelled to achieve a uniform tension across the cables.

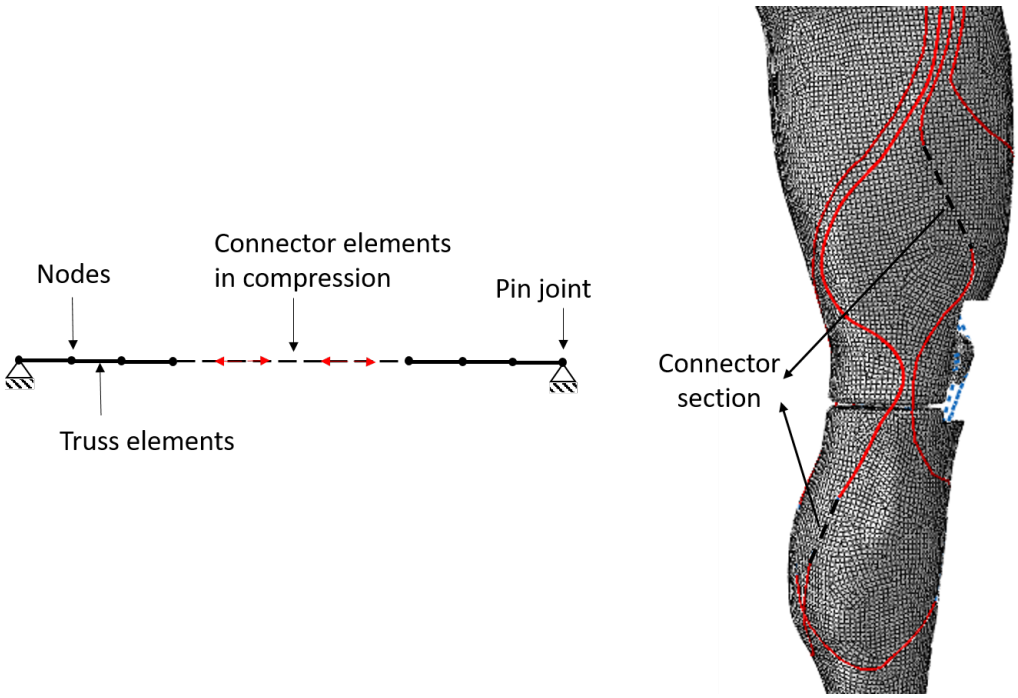

Figure 3.10: Pre-tension induced in cables using connector elements

Constraints and Interactions

Constraints in Abaqus can be used to define kinematic dependencies between the assigned nodes. The degrees of freedom at the dependant nodes are eliminated, constraining the relative motion between them. A TIE constraint was applied between various parts of the assembly to tie two surfaces or nodes such that there is no relative motion between them.

As described previously in the Section 2.3, one end of the cables in the knee brace is fixed to the waistband of the tight and the other end of the cables wrap around the dial to pull and lock the cable into tension. Therefore, in the model, a TIE constraint was applied to tie the end nodes of the cable to the top end of the leg. Rigid attachment of the leg to

the femur and tibia bones was achieved using TIE constraint. It was also used to enforce zero relative motion between the cable tubes and the external leg.

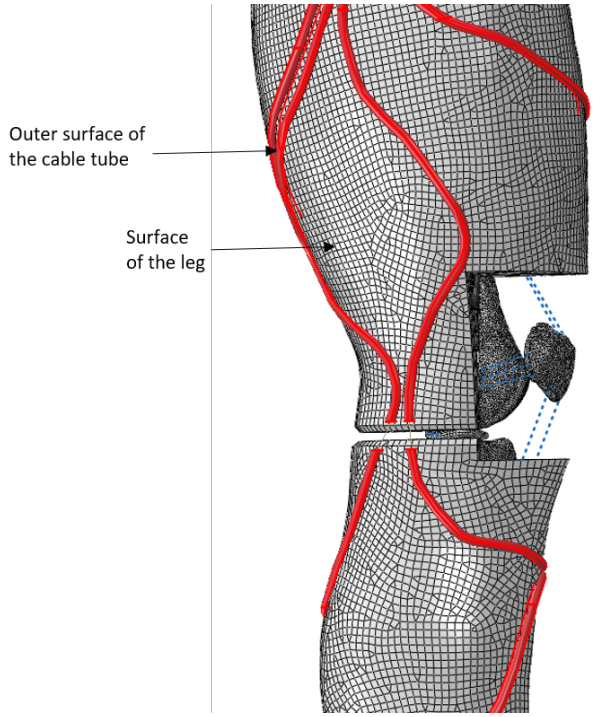

Figure 3.11: Tie constraint between leg and cable tubes

In the Explicit Dynamics module of Abaqus, the contact between various parts was defined using the Interactions module. In the tangential direction, a frictionless contact between the cables and the external leg or the cable tubes was given for free sliding of the cable over the leg (Figure 3.12).In the normal direction, a hard contact pressure overclosure method was used to prevent the penetration of cable nodes into the surface of the leg and the cable tubes. A General Contact was formulated for contact between the cables and the external leg/ cable tubes. A Contact Initialization was given between the cables and external leg to remove any initial surface overclosure of the cable nodes. This ensured that the cables did not go slack due to the nodal penetration of cables into the surface of leg/cable tubes and the pre-tension was maintained.

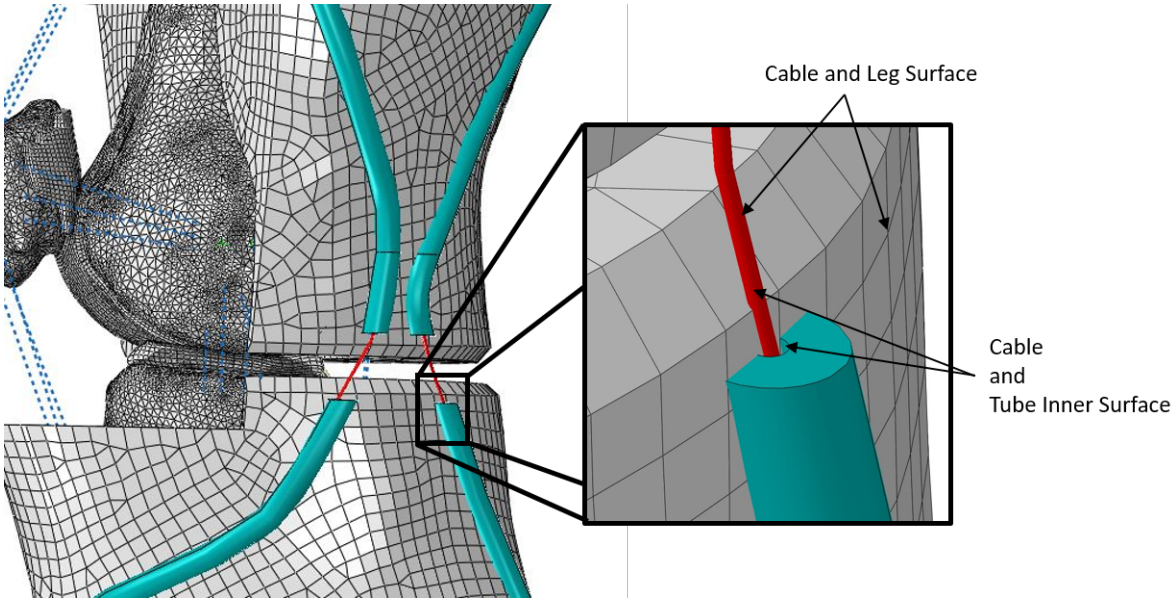

Figure 3.12: Frictionless contact between the cables and the leg/cable tube

Material Properties

Although, the material properties of the external leg were theorized to not contribute to the effective stiffness of the knee joint, a linearly isotropic material model of the external leg model was assigned similar to that of the surrogate leg used in experimental testing. An indenter test simulation in Abaqus was modelled similar to the experimental method. An arbitrary Modulus of Elasticity was given to the external leg. It was fixed at both ends and the bottom of the leg was constrained from movement. An indenter was then translated to cause an indentation of a pre-determined displacement. Force reaction at the indenter was simultaneously noted. The Modulus of Elasticity was changed until the force vs displacement values matched the experimental values. Based on this trial and error method, an approximate Modulus of Elasticity was calculated (E = 110 MPa, v= 0.45). In the knee brace model, because a set of four cables was modelled to be a single cable, the Modulus of Elasticity was multiplied by a factor of four to account for the indentation due to four cables. Test data from uniaxial tensile study on woven nylon conducted by Vlad and Oleksik (2019) was used to assume a linearly isotropic material model for the cables.

3.3 Finite Element Analysis

After the FE model of the knee brace on the knee joint was developed, it was validated using the experimental data study conducted in-house by the R&D Team at Stoko. Next, single leg jump landing simulations of ten participants were carried out on this model to predict the ACL behaviour with the knee brace on. Comparisons were made to the data from simulations conducted by Rao (2020) without the knee brace to evaluate its effectiveness.

3.3.1 Quasi-Static Analysis

To replicate the methodology of tests conducted experimentally, a quasi-static analysis was carried out in Explicit Dynamics module in Abaqus.

The reason for conducting a quasi-static analysis was to achieve a converged solution with the geometric, material and contact non-linearities, which would otherwise not be possible in a static step. Two approaches to obtain an economical solution was to introduce mass scaling to certain sections of the model with a smaller element size and increase the rate of loading in the model such that the inertial forces remained insignificant. The minimum stable time increment can be given by:

$$\Delta t = \frac{Le}{Cd}$$

where Le is the smallest characteristic element length and Cd is the wave propagation speed in the medium. Cd is calculated using the equation:

$$Cd = \sqrt{\frac{E}{\rho}}$$

E is the Modulus of Elasticity of the medium and ρ is the density of the material. Mass scaling technique scales the mass of the material by an assigned factor, hence increasing the density and thereby increasing the stable increment time. Mass scaling of factor 3 was given in the model to increase the mean stable time increment. Rate of loading in the simulation was increased to 600mm/sec.

To verify that the accuracy of the results was not compromised during the quasi-static analysis, the energy plots for the simulation were monitored. The kinetic energy plot was within 5% of the internal energy plot, indicating that the inertial effects were

negligible. One of the adduction simulations was also repeated with a reduced loading rate of 200mm/sec. Load vs. displacement response was compared (Figure 3.13) to the response with the higher loading rate to verify that the accuracy of results was not altered due to inertial effects.

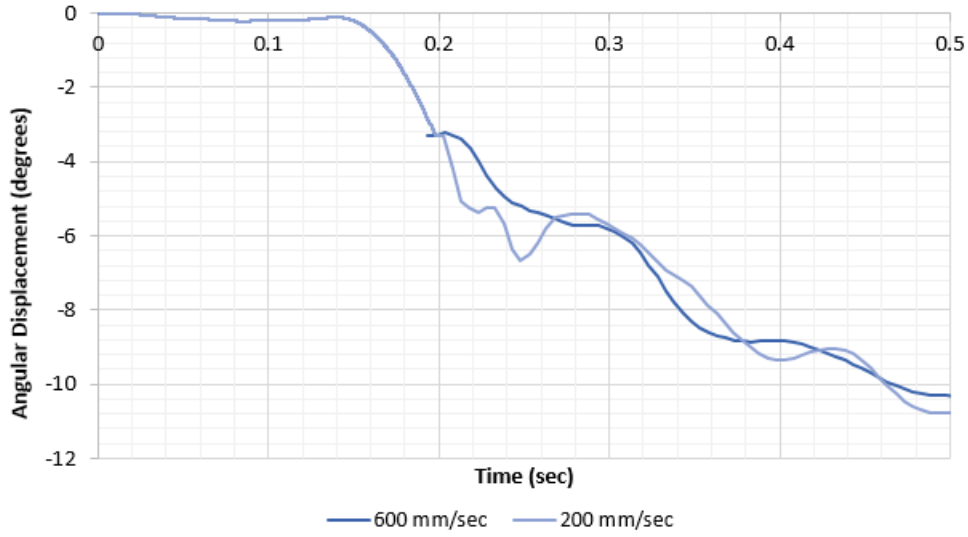

Figure 3.13: Comparison of angular displacement at different adduction speeds

3.3.2 Boundary Conditions for Adduction and Abduction

Similar to the experiments, the abduction and adduction motions were performed for 0 N, 14 N, 21 N and 35 N cable pre-tension values. Simulations without a knee brace on were also performed for both motions.

The simulations were conducted in three steps. In the first step, the pretension load was applied to the cables. This was done by applying a linearly ramped displacements of pre-determined values to each of the connectors to achieve a uniform tension of desired magnitude across the cables. The pull displacement values in each of these cables were calculated based on the strain (given by the ratio of stress and Modulus of Elasticity) applied to pull cable into the pre-determined tension. In the second step, a flexion angle of 20^o was applied. This was done by applying a quadriceps force of 800N while the hip joint was restricted from motion in all six degrees of freedom. In the last step, adduction or abduction moment ramped up linearly from 0 to 50 Nm was applied at the knee joint.

No muscle forces were applied at the leg in this step. The boundary conditions applied to the model are as shown in Figure 3.14.

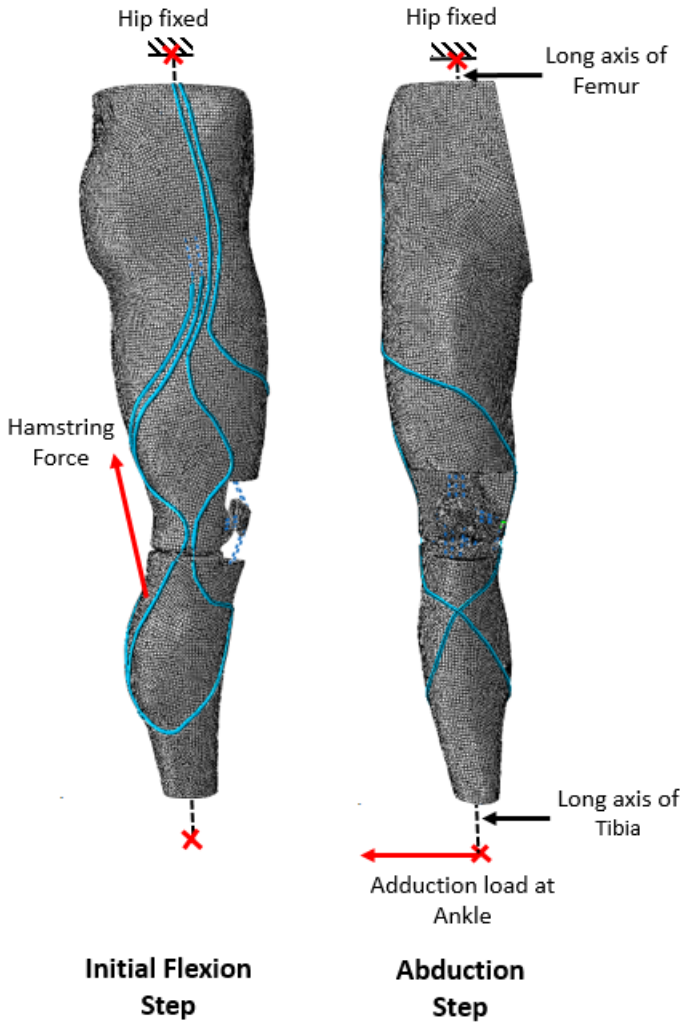

Figure 3.14: Boundary conditions for adduction/abduction motions

Displacement response at the ankle was recorded as the moment at the knee joint was ramped up. The load vs. displacement plot for each simulation were then compared to the experimental data.

3.3.3 Single-Leg Jump Landing

Although static analysis was conducted to evaluate the effectiveness of the knee brace, most injuries occur in dynamic loading conditions due to more complex injury mechanisms. Therefore, single-leg jump landing simulations of ten participants were conducted in braced configuration with the current FE model to observe the effects of the knee brace in dynamic loading conditions. Results were then compared to the jump landing computational study conducted by Rao (2020) in unbraced configuration to quantify changes due to the knee brace.

Jump landing kinematic and muscle force profiles of ten participants from Bakker (2014) were input as boundary conditions for the current study. Motion capture study was conducted by Bakker (2014) to collect kinematic data and ground reaction forces for all ten participants while they performed jump-landing motion. This data was then input in OpenSim software to calculate the dynamic muscle forces, hip flexion moments and kinematics of the hip and the ankle using inverse dynamics approach.

Jump landing simulations were conducted in three steps. In the first step, a pre-tension load of approximately 30N was applied uniformly to the cables in the knee brace. In the second step, an initial flexion angle to the knee was given based on the flexion angle of the participant when they made contact with the ground. The FE model of the knee in its original state was 12^o because this was the resting state of the cadaver on which the model is based while the MRI scans were taken. Considering this, application of initial flexion was not required in some participants. Jump landing was simulated in the third step. The duration of this step was 400ms. The first 100ms were the initialization of muscle forces, where they were ramped up linearly from 0. No kinematic input at the hip and ankle were given here. In the next 300ms, first 100ms were pre-ground contact and next 200ms were post-ground contact. A timeline of single-leg jump landing simulations is shown in Figure 3.15.

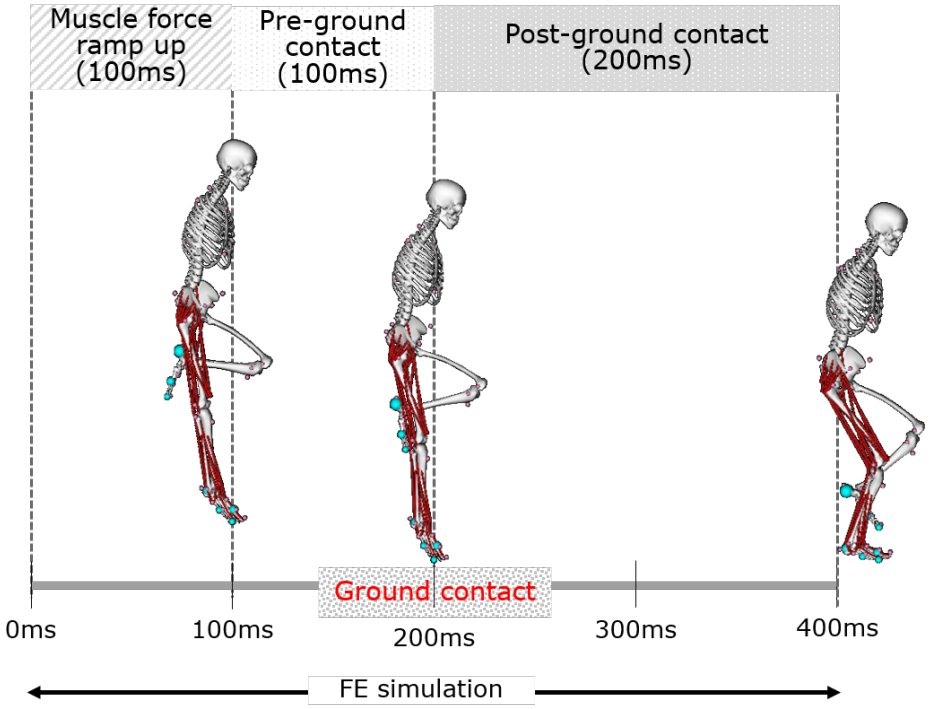

Figure 3.15: Timeline of single-leg jump landing simulations (Adapted from Rao (2020))

3.3.4 Boundary Conditions for Single-Leg Jump Landing

The transepicondylar axis connecting the lateral peak and medial sulcus of the femoral condyle was assigned the z-axis. The x-axis and y-axis were assigned such that they were parallel to the ankle and hip joints' translational directions as well as coincidental with the respective joints (Figure 3.16). The location of the hip and the ankle joint varied for each participant based on their limb lengths. Consequently, a coordinate system for each participant jump profile was created.

To achieve the initial flexion, the hip was translated in the y-axis while the tibia was restricted from motion. During the jump landing, velocity curves were applied at the hip and the ankle. The ankle was restricted from motion in the y-axis but free to rotate and translate in x-axis and z-axis. At the hip, rotation about the x-axis and the y-axis was restricted. Note that these boundary conditions were adapted from the jump landing simulations conducted by Rao (2020).

Figure 3.16: Coordinate system created for single-leg jump landing simulations (Adapted from Rao (2020))

Dynamic muscle forces were applied for the quadriceps, hamstring and gastrocnemius muscles. A hip moment was also applied at the hip joint. The quadriceps force was applied on three nodes at patella and the hamstrings force was applied on three nodes at the posterior tibia, line of action of both of which was parallel to the femoral axis. The gastrocnemius force was applied on three nodes at the posterior femur, parallel to the tibial axis. The locations of muscle force application were consistent for simulations of all ten participants as shown in Figure 3.17.

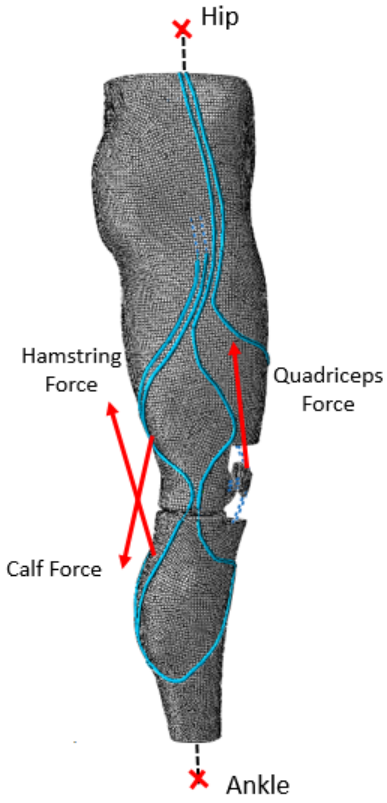

Figure 3.17: Boundary conditions for single-leg jump landing

An example of the input hip and ankle joint kinematics and muscle forces and hip moment plots if in Figure 3.18 and Figure 3.19 below.

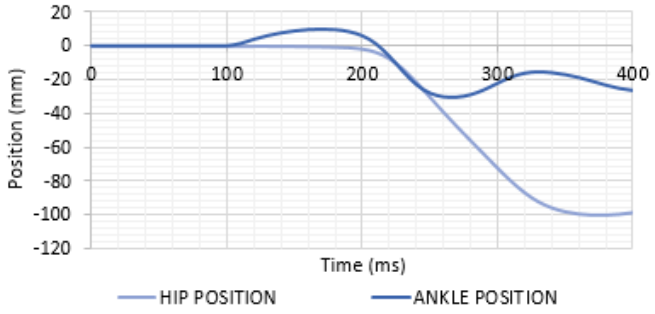

Figure 3.18: Hip and ankle kinematic boundary conditions of P1 participant

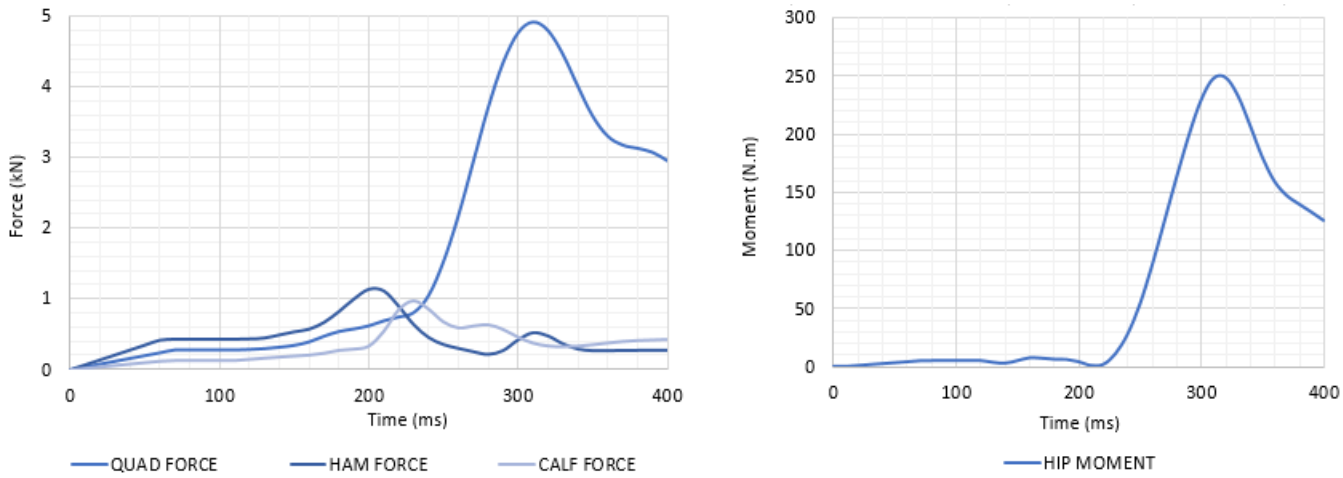

Figure 3.19: Muscle forces (left) and hip moment (right) of P1 participant

An axial force acting on the ACL caused a strain in the ligament. Similar to Rao (2020), the engineering strain in the ACL was calculated using the equation:

$$\epsilon = \frac{\Delta L}{L}$$

where L is the length of the AM bundle of the ACL (as shown in Figure 3.20)at ground contact and ΔL is the change in length of the AM bundle of the ACL relative to L. The ACL strain was plotted for the duration after the leg made contact with the ground which was the last 200ms of the total duration of the jump-landing simulations. Because the

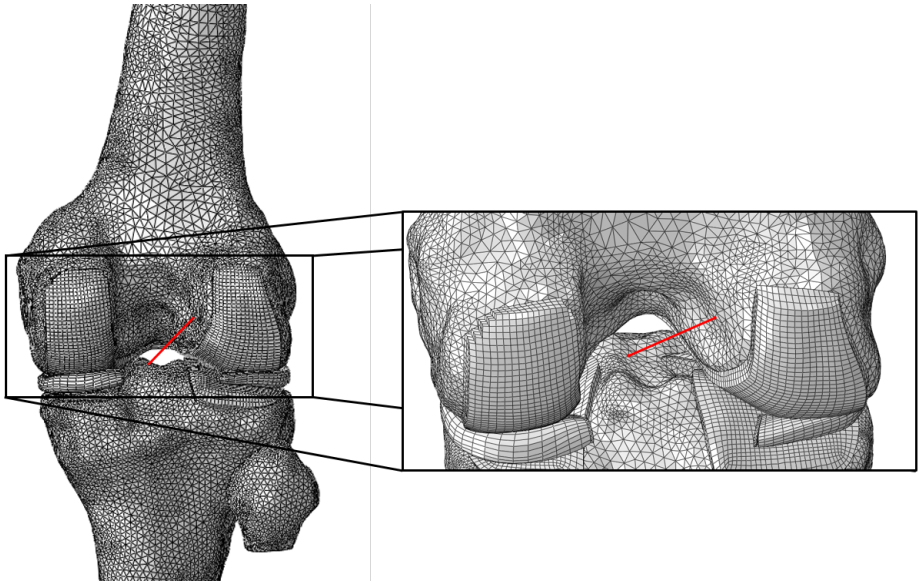

Figure 3.20: Anteromedial bundle of ACL in the FE model

initial length of the AM bundle of ACL was calculated after the muscle forces were ramped up and kinematic boundary conditions were applied, it varied between all participants.

Paired T-tests were conducted to compare the mean peak ACL strain and the mean time taken to peak the ACL strain for each participant in braced and unbraced conditions. This test was done to quantify the difference in the means due to the variability in the data. A confidence interval of 95% was used and the p values were calculated to determine if the difference between the means in braced and unbraced conditions were statistically significant. If $p > 0.05$, the difference in the means is not significant. If $p < 0.05$, it can be stated with 95% certainty that the difference in the calculated means is significant.

Chapter 4

Results

In this chapter, results of the simulations conducted on the FE model are discussed. An overview of mesh generation output is evaluated. Results from kinematic validation study are presented. Lastly, single-leg jump landing simulation results are presented and comparisons between braced and unbraced configurations are made.

4.1 Evaluation of Mesh Output

For the FE model, the leg was meshed with 4-node tetrahedral mesh, the cable tubes with 8-node hexahedral mesh and the cables with 2-node truss elements. Table 4.1 below provides an overview of mesh metrics.

Part	Mesh Type	Number of Elements	Number of Nodes	Element Size (mm)
Cable 1	Truss	329	330	4
Cable 2	Truss	321	322	4
Cable Tube 1	Hexahedral	14084	19565	2
Cable Tube 2	Hexahedral	13269	19152	2
Leg	Tetrahetral	997479	190684	4

Table 4.1: Mesh metrics

A summary of shape metrics is given in Table 4.2 below.

Part	Average Minimum Angle	Average Maximum Angle	Aspect Ratio	Geometric Deviation Factor
Cable 1	-	-	-	0.0062
Cable 2	-	-	-	0.00687
Cable Tube 1	59.53	125.38	2.55	0.0877
Cable Tube 2	58.25	127.86	2.28	0.0915
Leg	36.30	89.32	1.76	-

Table 4.2: Shape Metrics

Default values from Abaqus were used to assess the mesh quality of all elements. For hexahedral elements, the acceptable minimum quad-face corner angles were 10 and 160 degrees respectively. The aspect ratio should be below 10 and the geometric deviation factor below 0.2. For tetrahedral elements, acceptable ranges for quality assessment parameters are same as hexahedral elements, except for an additional parameter where tet-face corner angle can be between 5 and 170 degrees.

4.2 Quasi-Static Validation Study

Validation study of the knee brace was conducted in abduction and adduction loading conditions. Simulations were conducted to replicate the experimental testing methodology. Moment versus angular displacement responses were generated and compared to the experimental results.

4.2.1 Experimental Study

Average reaction torque at the knee versus angular displacement plots from the experiments are as shown in the Figure. A 9° angular displacement was given and torque reaction at the knee was recorded. Curves for four values of pre-tension were plotted where the baseline curve is at 0N, using which the load reduction was calculated. Figure 4.1 and Figure 4.2 show the response of the knee brace in valgus and varus respectively from experiments.

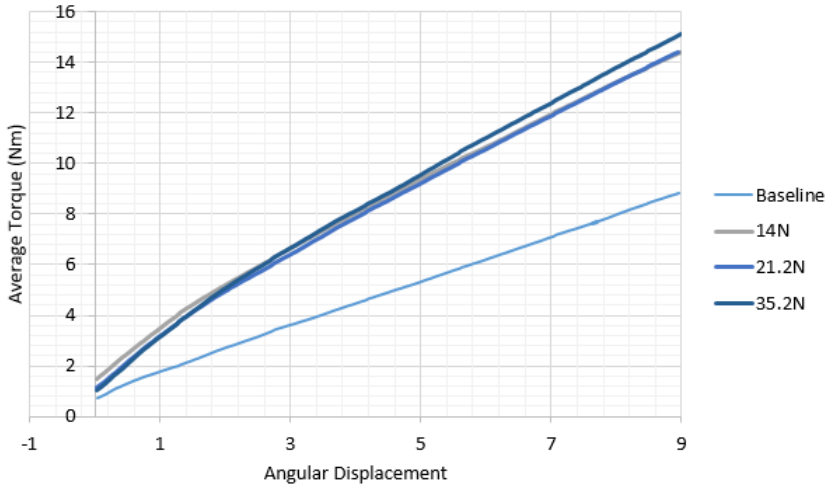

Figure 4.1: Load versus angular displacement curve in valgus (Experimental Analysis)

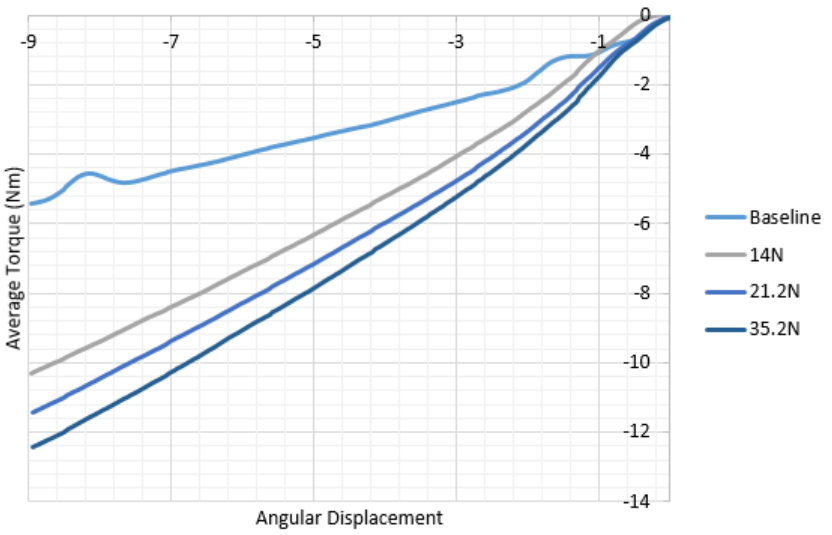

Figure 4.2: Load versus angular displacement curve in varus (Experimental Analysis)

4.2.2 Computational Study

Results of moment versus angular displacement curves for the simulations of valgus and varus are shown in Figure 4.3 and Figure 4.4 respectively. A linearly ramped up moment up to 50 Nm was applied and the angular displacement was recorded.

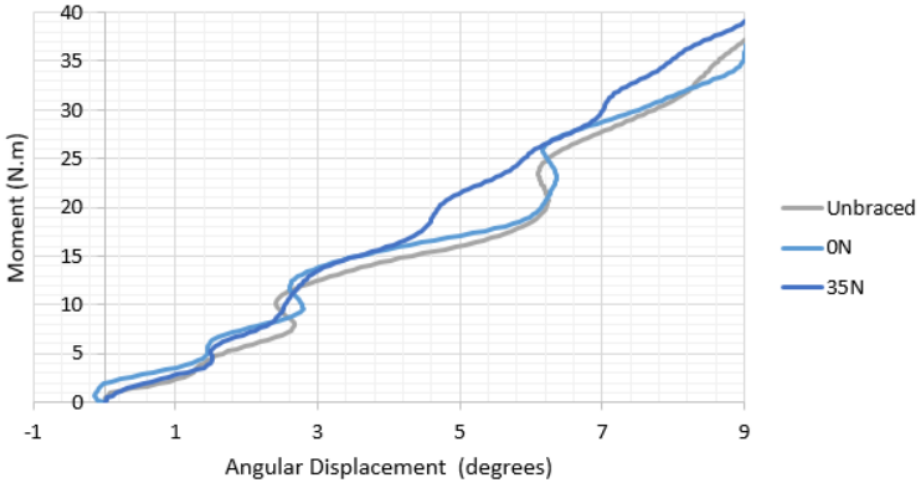

Figure 4.3: Load versus angular displacement curve in valgus (Computational Analysis)

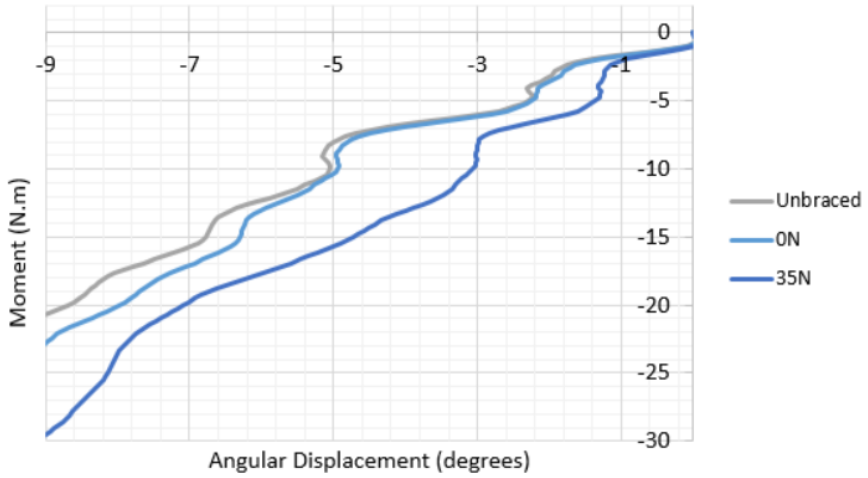

Figure 4.4: Load versus angular displacement curve in varus (Computational Analysis)

The absolute reduction in torque at the knee with the application of 35N pre-tension was calculated from the baseline (0N pre-tension). Load reduction was calculated at 9 degrees of angular displacement in both varus and valgus. Comparison was made between experimental and computational results, as shown in Figure 4.5 below.

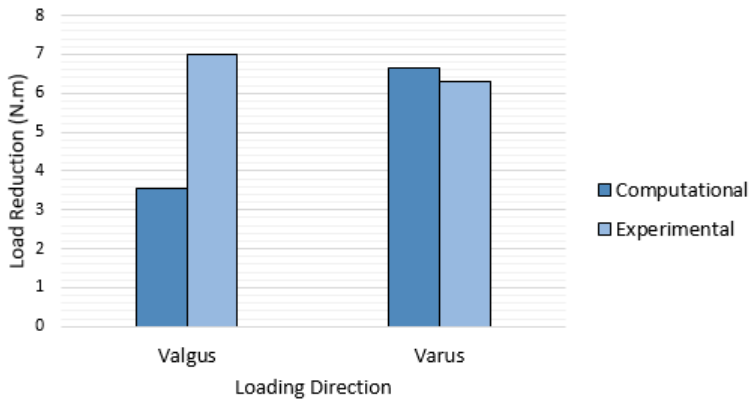

Figure 4.5: Comparison of load reductions between experimental and computational analysis

Similar to the load reduction, the reduction in angular displacement was found for 35N cable pre-tension in comparison to the baseline at 0N pre-tension in the cables in Figure 4.6.

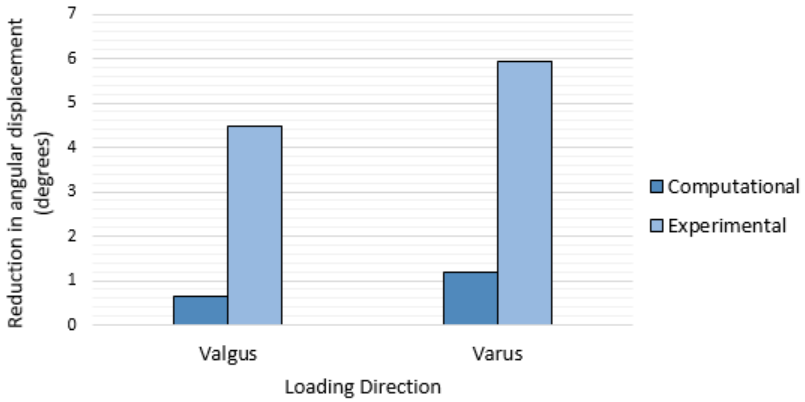

Figure 4.6: Comparison of displacement reductions between experimental and computational analysis

4.3 Single-Leg Jump Landing Study

Single-leg jump landing simulations of ten participants were conducted in braced and unbraced configurations. ACL strains for each participant were plotted for the duration of simulation after ground contact has been made. This time period was the last 200ms of the total length (400ms) of the jump landing simulation.

4.3.1 ACL Strain Behaviour

ACL strains of all participants with and without the brace are plotted below in Figure 4.7.

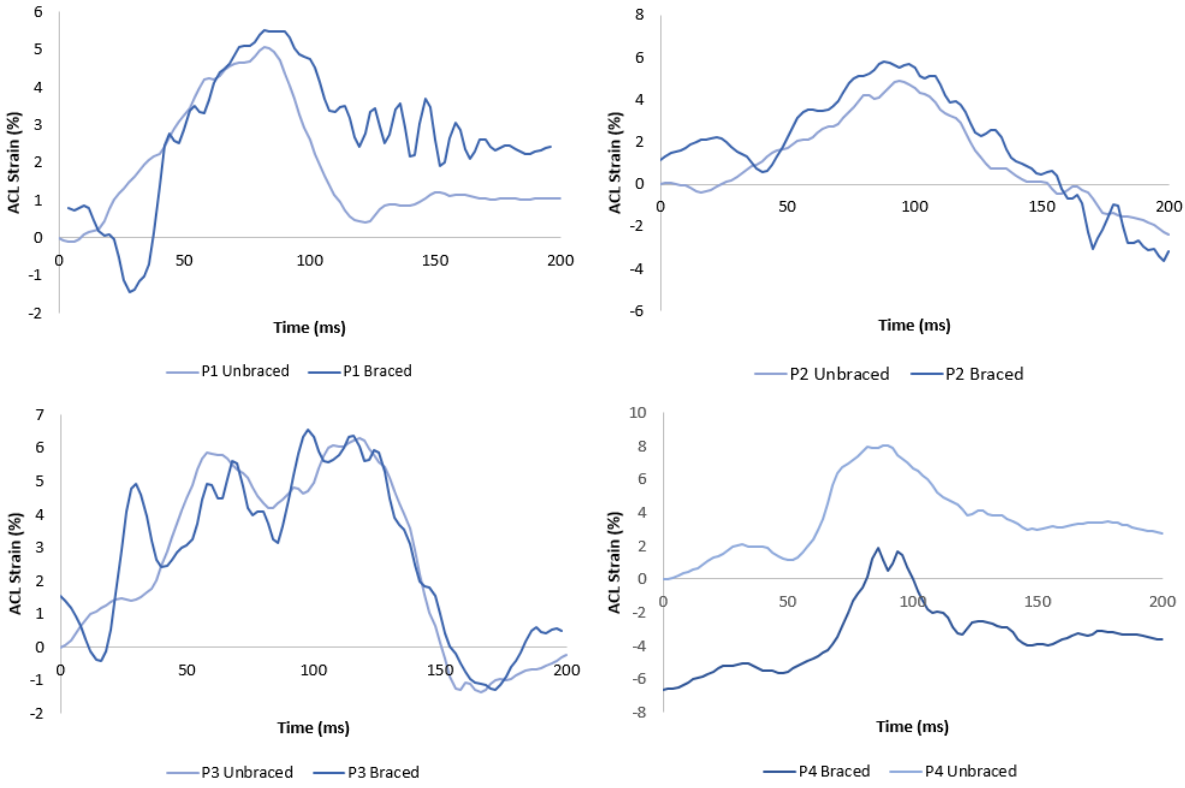

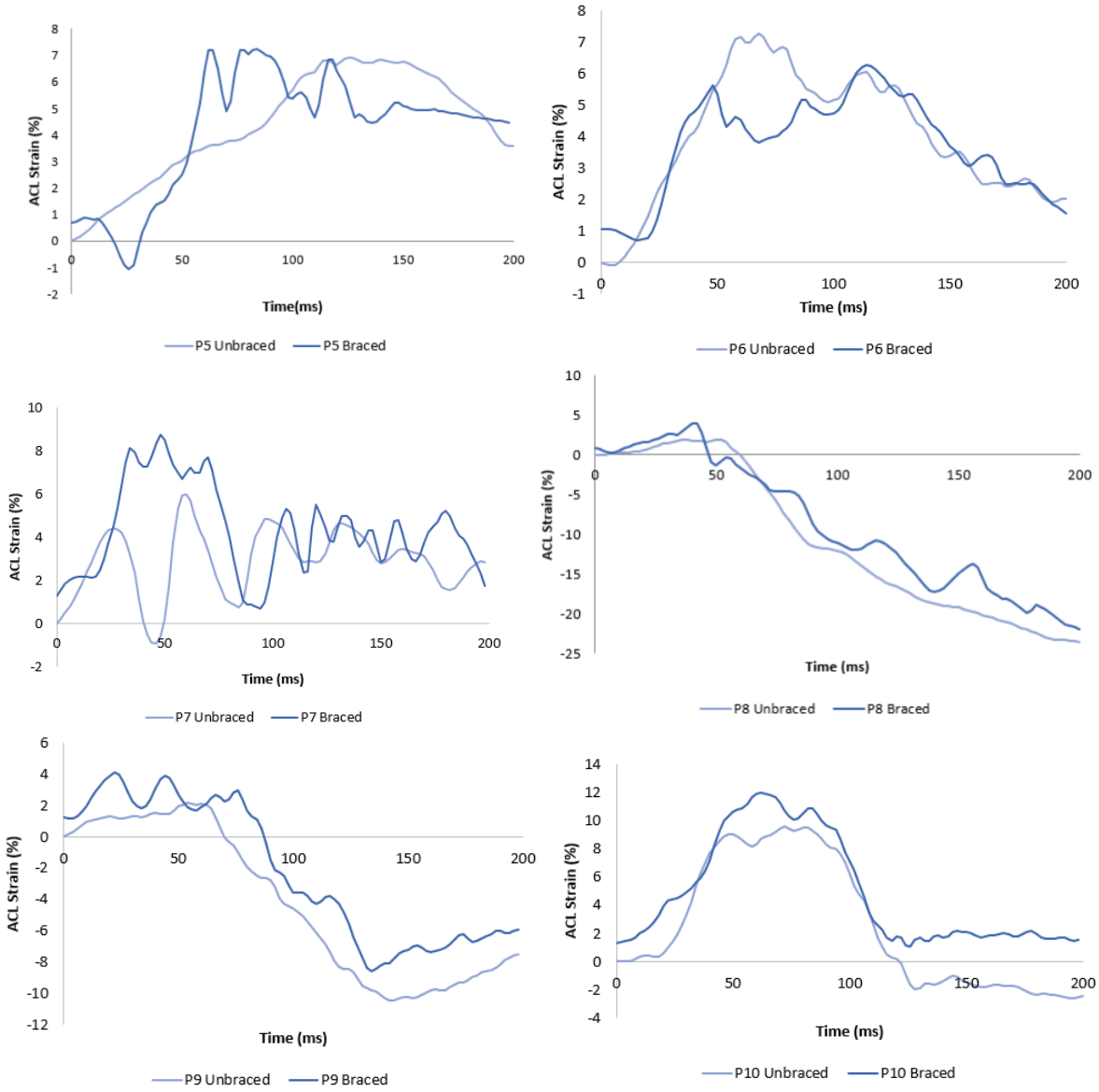

Figure 4.7: ACL strains of P1-P10 in unbraced and braced configurations

Comparison of the peak ACL strains(%) and the time taken for strain to peak between braced and unbraced configurations for all participants are shown in Figure 4.8 and Figure 4.9 respectively.

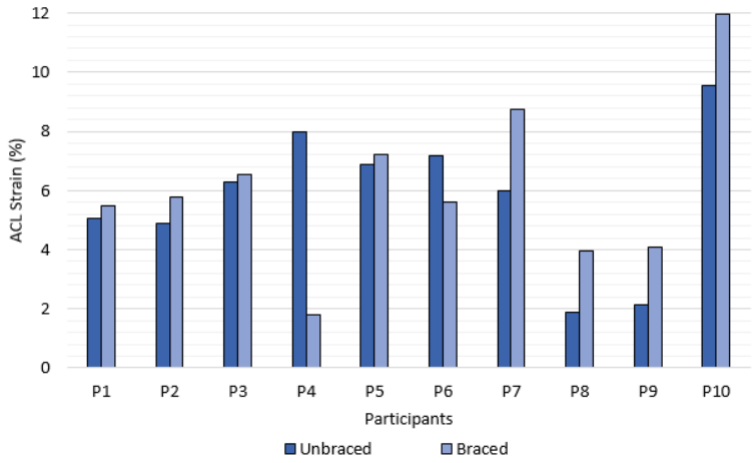

Figure 4.8: Comparison of peak ACL strains in P1-P10 in unbraced and braced configuration

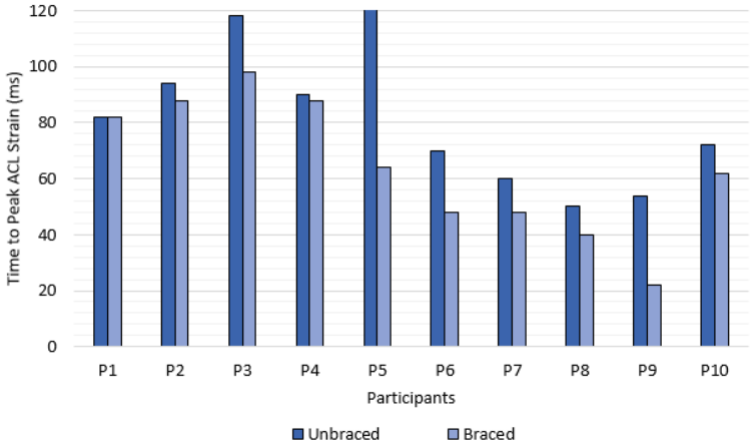

Figure 4.9: Comparison of time taken for ACL strains to peak in P1-P10 in unbraced and braced configuration

4.4 Energy balance

Explicit Dynamics method can be used to solve highly non-linear static problems which are otherwise difficult to converge in using static analysis. The sources of non-linearity could be geometry, material constitutive models or contact. Additionally, computational time may increase with use of Implicit Analysis as model becomes more complex. Hence, a quasi-static approach was executed using Explicit Dynamics. As discussed in Section 3.3.1, to obtain an economical solution, the speed of the analysis was increased and the mass of the model was scaled up.

Energy balance equation was used to verify that the response generated from the quasi-static analysis were accurate. The equation can be given as:

$$E_{Total} = E_{Internal} + E_{Kinetic} + E_{Viscous} - E_{External} = CONSTANT$$

To examine that the results from the analysis reflect a quasi-static solution, the kinetic energy should be less than 5% of the internal energy. Also, the total energy should be approximately constant to obey the law of conservation of energy.

Energy plots for simulation of adduction in 35N cable pre-tension and for one of the participants during single-leg jump landing in braced configuration is shown in Figure 4.10.

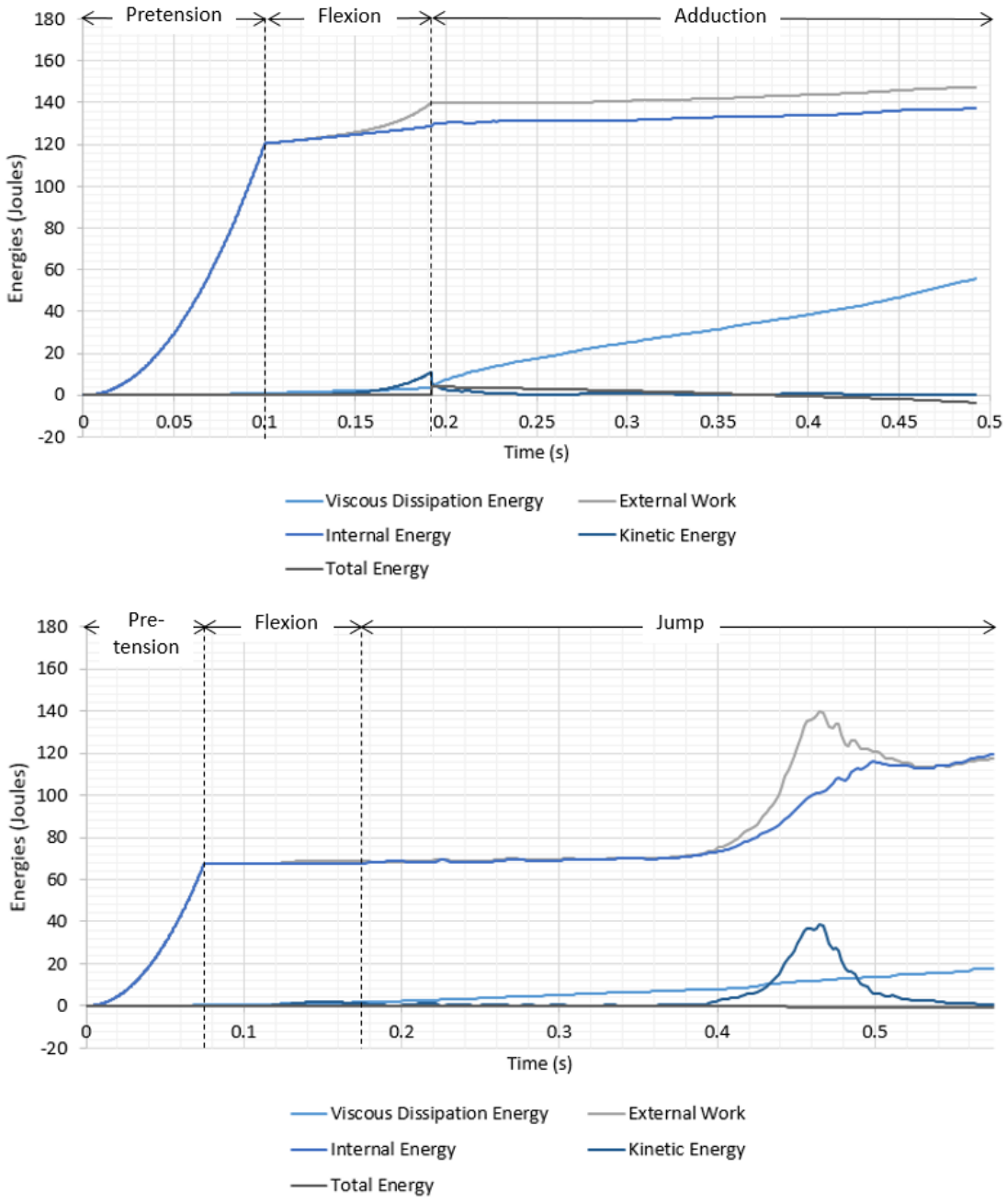

Figure 4.10: Energies of the simulation during braced adduction with 35N cable pre-tension (top) and during braced single-leg jump landing for P10 (bottom)

Chapter 5

Discussion

A number of studies have been conducted to evaluate the effectiveness of knee braces experimentally (Paulos et al. (1991), Baker et al. (1989), Meyer et al. (1989), Erickson et al. (1993)) in static and quasi-static loadings. Few researchers have also applied computational methods to test and optimize knee braces (Haris and Beng Chye Tan (2021), Pierrat et al. (2014), Pierrat et al. (2015b)) in quasi-static conditions. However, most ligamentous injuries occur during dynamic scenarios for which very few studies have been conducted (Hangalur (2014)). To our knowledge, this is currently the only study that used computational analysis to quantitatively evaluate the effectiveness of a knee brace during both quasi-static and dynamic loading scenarios. This allowed for assessment of ACL strain behaviour with and without knee brace by simultaneous input of muscle forces and joint kinematics on an anatomically accurate knee.

The purpose of this study was to evaluate the effect of mechanical design of a cable stabilized brace on ACL behaviour during single-leg jump landing activity. The knee brace is one of a kind, using a system of non-extensible tension cables running through a compression tight to provide mechanical stability to the knee. FE model of the knee brace was developed on an existing FE model of a subject-specific knee. Cabling pathways of the brace were identified and an external leg was modelled for the cabling system to be mounted on. Created model was validated in quasi-static loading using data available from experimental testing. Single-leg jump landing simulations were conducted for jump profiles of ten participants in braced configuration. Muscle forces and joint kinematics for jump profiles were input from Bakker (2014). These results in braced configuration were compared to results in unbraced configuration from study conducted by Rao (2020).

5.1 Development of Knee Brace FE Model

Modelling strategy was developed to accurately model the knee brace while also simplifying the model design. In the current study, external leg was modelled in a similar way devised by (Hangalur (2014), Erickson et al. (1993)), encompassing the knee model on which the cabling system was mounted for performing analysis. Because of the unavailability of the MRI scans of entire length of the subject's leg on which the knee model is based, an open source geometry of leg was used and modified to conform to the size of the knee. MRI scans of the knee joint were referenced to scale and position the encompassing leg over the knee. The leg was also partitioned in the middle (Figure 3.5) to allow for flexion and extension motions by preventing the addition of stiffness to the knee from the leg. Otherwise, the region of the leg at the knee created a lever at the knee medially, causing the femur to pivot about it unnaturally. The geometry of the leg was not critical in effecting the mechanics of the knee brace and it was developed solely for the purpose of mounting the cables and restricting them from going slack.

The cables in the cabling system run along pre-designed complex pathways in the knee brace. For modelling of these cables, the coordinates of their pathways were tracked manually based on visual inspection. This approach was justified because their coordinates relative to the knee vary across users. Moreover, for the same user, the absolute coordinates of these pathways will be different every time user puts on the knee brace.

In the cabling system, eight cables run which diverge into set of two with four cable in each. A set of these four cables was modelled as a single cable in the model (Figure 3.7). This allowed for a reduced computational time by reducing the number of contact pairs between the cables and the leg and the cables and the cable tubes. The applied tension in cables in the simulations was therefore four times the value of the tension measured experimentally.

Cables in the knee brace were non-extensible tension cables and in compressive loading they become slack. The cables modelled in the FE model were meshed with truss elements and strategized to be formulated for no compression. As a limitation of Explicit Dynamics algorithm of Abaqus, the truss elements could not be modelled for no compression and it was allowed in the cables. However, the compressive stresses in the cables were negligible compared to the tensile stresses in all simulations and analysis. Also, compressive stresses were lower because slacking was allowed at the partition of the external leg.

5.2 FE Model Validation Studies

To quantify the mechanical stability provided by the knee brace, the FE model of the knee brace was tested in quasi-static varus and valgus loadings. The results were compared to data from tests conducted experimentally with a surrogate leg and Knee Testing Fixture by the team at Stoko. The effective load versus angular displacement (Meyer et al. (1989), Baker et al. (1989), Pierrat et al. (2015b)) was used as a measurement to compare the braced and unbraced conditions.

For both varus (Figure 4.4 and 4.2) and valgus motions (Figure 4.3 and 4.1), similar trends were observed and the hypothesis in Section 3.1.2 was proved. The load reductions at the knee for valgus and varus were recorded between 0N and 35N cable pre-tension conditions. With the increase in cable pre-tension, a greater load reduction was seen.

Experimentally, the load reductions were 7 Nm and 6.3 Nm in valgus and varus respectively as compared to the computational analysis where they were 3.5 Nm and 6.66 Nm. The load reductions were similar for varus. However, the recorded load reduction for valgus was lower in computational analysis. The reduction in the angular displacement corresponding to maximum moment at baseline was 65.7% and 49.7% for varus and valgus experimentally, which were much higher than the computational results with 13.33% and 7.0% for varus and valgus respectively. This variation in the reduction in angular displacements was attributed to the low stiffness of surrogate leg as compared to that of the FE knee model. The knee valgus versus abduction moment plot in Figure 5.1 from Kiapour et al. (2014), using which the knee model was validated in valgus by Rao (2020) shows the change in moment at the knee required to achieve a desired change in angular displacement. A higher pre-tension value in the cables, based on the stiffness of the knee, could reduce the angular displacement in the knee substantially, decreasing the chances of injury to the knee.

Paulos et al. (1991) evaluated knee braces in a lateral impact loading using a surrogate leg. They reported a reduction in the peak ACL and MCL strains. Similar to the current study, they concluded that the net moment at the knee joint reduced due to mechanical restraint of the knee brace.

Baker et al. (1989) conducted also conducted study on prophylactic and functional knee braces for abduction loading at various flexion angles, a loading condition similar to the current study. They reported a reduction range of 0-22% in abduction angle with the same load based on several knee braces. The results of the current study as well lie in this range.

The reduction in effective load at the knee with increasing cable pre-tension was not as high in valgus compared to varus, as observed from both computational and experimental

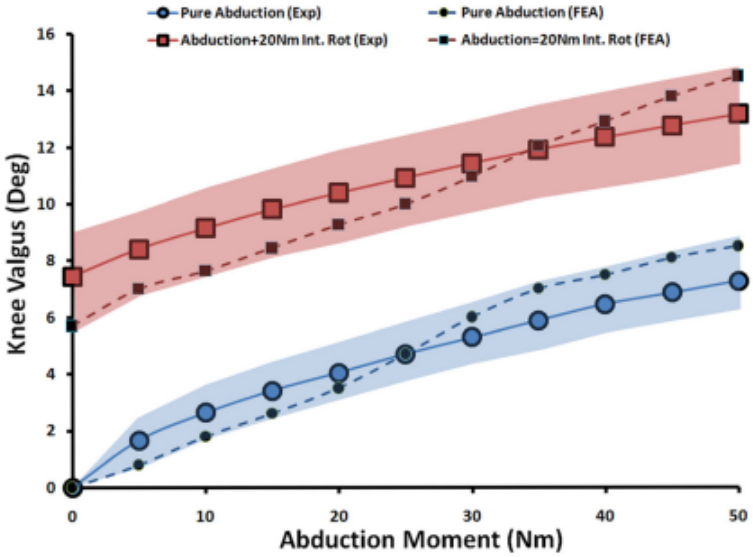

Figure 5.1: Abduction moment versus Knee valgus curve (Adapted from Kiapour et al. (2014))

analysis (Figure 4.1 and 4.3). Also in valgus, the plots of moment vs angular displacement in unbraced and 0N pre-tension conditions have a small difference (Figure 4.3) and the behaviour is different compared to varus. An explanation for this is that in the current FE model of the knee, the stiffness of the MCL and LCL are different, stiffness of the MCL being higher than the LCL. This difference can also be noted from Figures 4.3 and 4.4, showing a higher force required to in valgus compared to varus to achieve the same value of angular displacement.

Also, in case of 0N pre-tension simulations, the tension in the cables increases with the increase in angular displacement. However, it was noted that the increase in tension in the cable was much higher laterally (in varus) than medially (in valgus). This behaviour could be attributed to the unsymmetrical design of cable pathways running medially and laterally.

5.3 Single-Leg Jump Landing Simulations

In the past, researchers have taken the approach of using experimental in-vivo and in-vitro methods to study the behaviour of ACL during dynamic loading. In-vivo measurement of

ACL strain by Beynnon et al. (2003) made use of transducers applied the ligament. However, such techniques are invasive and pose ethical issues associated with them. Researchers have also made use of EMG (Taylor (2011), Ramsey et al. (2003)), Osternig and Robertson (1993)) and motion capture (Hashemi et al. (2010), Shuaib et al. (2014), Taylor, Yeow) to derive ACL strains. In-vitro simulation using cadaver and surrogate legs (Hangalur (2014), Erickson et al. (1993)) have also been employed for dynamic load testing. Experimental methods are strenuous with data collected for a small samples. Also, because of the mechanical design of the knee brace with a compression tight and tensioning of the cables, use of cadavers was not a suitable method. Therefore, in the current study, a computational model was used which allowed for extraction of ACL strains from an anatomically accurate knee model and replication of dynamic movements from multiple participants in real-time.

To test the effect of knee brace on the ACL, jump-landing simulations were conducted using the FE model. Jump profiles from Bakker (2014), including hamstrings, calf and quadriceps muscle forces, ankle and hip joint kinetics and kinematics, were input. ACL strain behaviour was then compared to the simulations conducted for jump landing in unbraced knee. Strain trends seen for different participant profiles were different due to the varying flexion angles and distinct landing strategies at ground contact across participants.

ACL strain and the time taken for the ACL strain to peak, being the critical parameters for ACL injuries (Rao (2020), Bakker (2014), Hangalur (2014)), were recorded to quantify the ACL behaviour in the current study. Comparison of the peak ACL strains in the braced and unbraced configurations are shown in the Figure 4.8. Observing the peak ACL strain curve post ground contact, a mean increase in strain values by 1.51% (p=0.01) in braced configuration was noted compared to the unbraced configuration as shown in Figure 5.2.

Because the knee brace evaluated in the current study is unique, a direct comparison with other studies conducted for braced jump-landing could not be made. In a unique method combination of in-vivo and in-vitro methods, Hangalur (2014) collected motion capture data for jump-landing with and without braced which was then input to DKS for simulation to measure the ACL strains in a cadaver knee. No significant reduction in ACL strain was noted solely because of the mechanical restraint provided by the knee brace. With the isolated effect of mechanical stabilization of the knee brace in the current study, an increase in the ACL strain is observed. However, it is relatively low, similar to the results of Hangalur (2014). Likewise, Erickson in their study concluded that although the overall impact force decreased at the knee, no reduction in the ACL strain was observed due to the effect of knee brace.

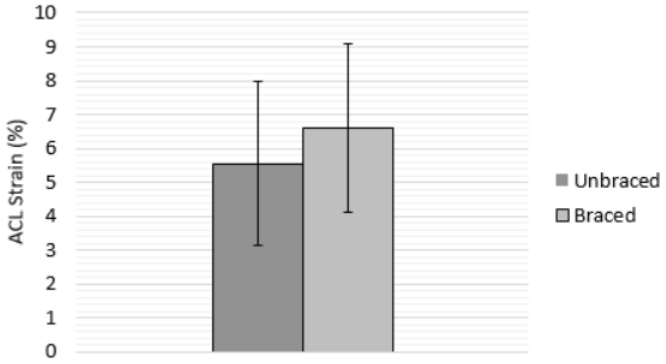

Figure 5.2: Comparison of mean ACL strain in unbraced and braced configuration

A mean decrease of 15.5 milliseconds was recorded in the time taken to peak the ACL strain as shown in Figure 5.3.

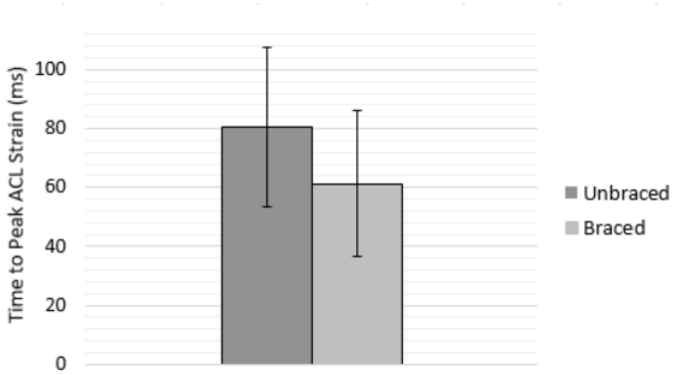

Figure 5.3: Comparison of mean time taken to peak ACL strain in unbraced and braced configuration

While a mean increase in the ACL strain was seen among participants, a decrease by approximately 6% was observed in P4, making it an outlier. A decrease in the ACL strain was noted in braced condition during muscle force ramp up period, which can also be noted in the Figure 5.4 where the value of ACL strain is decreased at the moment of ground contact.

Although the knee brace shows an increase in the ACL strain, it is not substantial to cause concerns. In a study conducted by Chandrashekar et al. (2005), the failure in the

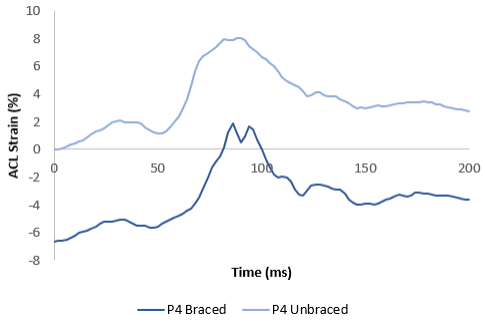

Figure 5.4: Braced vs Unbraced configurations in P4

ACL occured at 30% and 27% in males and females respectively (Figure 5.5. Compared to this, the mean increase in the ACL strain is 1.51% which is a relatively small increase to cause an injury. It is also possible that the strain in other ligaments such as the MCL and LCL decreased at the cost of a small increase in loading on the ACL, which can be further studied.

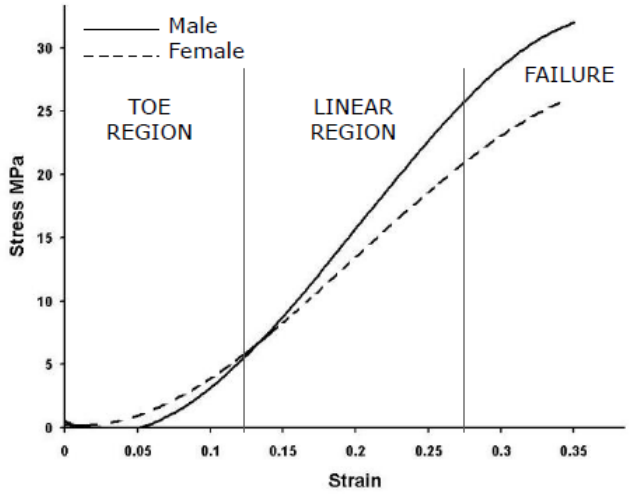

Figure 5.5: Stress-strain relationship for ACL (Adapted from Chandrashekar et al. (2005))

It is known that wearing knee braces alter the muscle activity in the knee. During the activity of running, Osternig and Robertson (1993) noted that the application of knee brace changed the neuromuscular activity causing the muscle forces to reduce between 67-83%. Likewise, Ramsey et al. (2003) and Hangalur (2014) had similar results where

they concluded that the increased stability in the knee during gait motion was due to changed muscle activity instead of the brace mechanics. This was not within the scope of the current study, however further studies are necessary to evaluate the proprioception effects to truly understand the effectiveness of the knee brace.

Chapter 6

Conclusions

6.1 Summary

The objective of this study was to evaluate the effectiveness of a cable stabilized knee brace, inspired by Stoko, in adduction/abduction motions and its effect on Anterior Cruciate Ligament (ACL) behaviour under dynamic loading. In the current study, a computational approach was taken to assess the knee brace and a Finite Element model of the knee brace was developed on an existing FE model of an anatomically accurate knee developed by Rao (2020).

The knee brace provides mechanical stability to the knee using a system of non-extensible pre-tensioned cables running a compression tight along designed pathways. The external leg and the cabling system were the two components of the knee brace model. An open source model of a human leg was processed to create a solid model of the leg which was further modelled to accurately position over the knee. The leg model was then meshed in Hypermesh. The cabling system in the model further consisted of the cables and the cable tubes which were modelled and meshed in Abaqus.

The developed FE model was validated in quasi-static adduction and abduction loading conditions by comparing the effective load reduction between the 35N and 0N cable pre-tensions at the knee to available experimental data. The experiments were conducted by the team at Stoko on the Knee Testing Fixture and a surrogate leg developed in-house. Based on computational results, the reduction in load was 3.5 Nm and 6.66 Nm in abduction and adduction respectively and the corresponding reduction in angular displacement was 7.0% and 13.33%. The data for load reduction compared well with the experimental data.

The hypothesis that the effective load at the knee would be reduced with increasing knee brace cable pre-tension was proven true. This indicated that the knee brace reduced the chances of injury in varus nad valgus loading conditions.

Single-leg jump landing simulations for ten participants were conducted in braced configuration, and compared against the results of unbraced configuration conducted by Rao (2020), to quantify the ACL behaviour with the knee brace. The muscle forces and joint kinematic and kinetic data for jump landings were input as boundary conditions. Peak ACL strain and the time taken for it to peak after ground contact were recorded. During the jump-landing activity, the mean ACL strain in braced configuration increased to 6.59 $\pm$2.49% from 5.54 $\pm$2.41% ($p = 0.024$) in unbraced configuration. The mean time taken for ACL to peak decreased from 80.66 $\pm$27.14 ms in unbraced configuration to 61.33 $\pm$24.61 ms ($p = 0.007$) in braced configuration. It was concluded that the ACL strain increased due to the mechanical design of the knee brace. The time taken to peak the ACL strains reduced. These parameters indicate that the chances of injury to the knee increased. However, the increase in strain is much lower than the failure strain in the ACL. Further studies are necessary to see the effect of the knee brace on the neuromuscular activity and changed muscles forces in participants to draw a conclusion on effectiveness of the knee brace. Also, the effect of knee brace on other ligaments such as the MCL and LCL needs to be studied.

In summary, computational evaluation of the mechanical stabilization effects of the knee brace in both quasi-static and dynamic loading conditions was employed. An approach to a more detailed study on the ACL, experimental analysis of which has its inherent challenges, was explored with the use of Finite Element Analysis. This study has also opened opportunities for potential future studies on knee braces and ability to isolate the effects of various parameters that effect knee stabilization.

6.2 Limitations

1. The results of the FE model of the knee brace were compared to the experimental data for motions only in the frontal plane (adduction and abduction). However, the model was not validated in the sagittal plane because of lack of experimental data available which is a limitation of the current study. Validation can be done by comparing data for motions in the sagittal plane from the KTF to the data from the FE simulations.

2. Computational time in simulations increased with the addition of a solid model of the leg. The major reason for the modelling of the leg was to mount the complete length of the cabling system. However, an alternate method of variable mesh generation could be

employed to reduce the computational time. A hollow and rigid external leg could also be modelled if a correct contact formulation between rigid body and truss elements can be conceptualized.

3. The model of the external leg used on the knee did not belong to the cadaver specimen on which the knee model was based. The MRI scans of the cadaver leg were not available for the complete length of the model, hence an open source geometry of the leg was processed and scaled based on approximation, by referencing the MRI images. Similarly, the cabling system was also based on visual approximation. A more precise technique for modelling the cable pathways like the use of digitization of the pathways and use of the leg of the cadaver would produce more accurate results. However, the results for load reduction at the knee agreed well with the experimental data.

4. Multiple sections of cables were modelled using connector elements instead of truss elements to achieve a cable pretension. A contact between these connector elements and the external leg could not be defined in Abaqus, implying missing sections of cables. This has a potential to introduce kinematic inaccuracies in the model.

5. Cable tubes were modelled to constrain the cables and introduce uniform stiffness in them. However, because the cables were modelled as wires, they had some allowance for going slack within the inner diameter of the cable tube. This could be a reason for slightly varying pre-tension along the complete length of the cables.

6.3 Future Work

1. The input boundary conditions for the dynamic loading simulations without the knee brace were used which isolated the effect of the mechanical design of the knee brace on the ACL. However, changes to the muscle firing patterns due to application of knee brace were not taken into account because of lack of availability of this data. To evaluate the true effect of the knee brace on the knee stability, inclusion of changes to neuromuscular patterns is necessary. One way to achieve this is by employing the experimental method of collecting motion capture data for participants while they perform jump landing activity with the knee brace on. Jump profiles collected thus can further be used to simulation jump landings computationally.

2. The effect of the knee brace on ACL was studied but the other ligaments such as the MCL and the LCL were not studied. Although an increase in the ACL strain was seen, the increase was relatively low. It is possible that the knee brace provides more stability to other knee stabilizing ligaments at the cost of a small increase in the ACL strain. Further

investigation can be done into this by validating other ligaments in the FE model against published data. Accurate comparisons in their behavior between braced and unbraced conditions can be made to understand the effects of the knee brace on other ligaments.

3. The change in kinematics of the knee with the knee brace was not studied in the current study. Validation of the knee brace model in the sagittal plane and the transverse plane can be done and used to further study its effect on kinematics of the knee in the three anatomical planes.

References

A biomechanical study of the static stabilizing effect of knee braces on medial stability. *The American Journal of Sports Medicine*, 15(6):566–570, 1987. ISSN 15523365.

S. Akizuki, V. C. Mow, F. Müller, J. C. Pita, D. S. Howell, and D. H. Manicourt. Tensile properties of human knee joint cartilage: I. influence of ionic conditions, weight bearing, and fibrillation on the tensile modulus. *Journal of Orthopaedic Research*, 4(4):379–392, 1986. doi: 10.1002/jor.1100040401.

J. P. Albright, J. W. Powell, W. Smith, A. Martindale, E. Crowley, J. Monroe, R. Miller, J. Connolly, B. A. Hill, and D. Miller. Knee Sprains in Effectiveness of Preventive Braces. *The American Journal of Sports Medicine*, 22:12–18, 1994.

R. S. Alexander Mitrichev and M. D. Wilson. The Extrinsic and Intrinsic Factors Predisposing to ACL Injuries in Female Athletes - Sports Medicine Implications in 2021. *Acta Scientific Orthopaedicse*. ISSN 2581-8635.

G. Anderson, S. C. Zeman, and R. T. Rosenfeld. The Anderson knee stabler. *Physician and Sports Medicine*, 7(6):125–127, 1979. ISSN 00913847. doi: 10.1080/00913847.1979.11710882.

S. Avril, L. Bouten, L. Dubuis, S. Drapier, and J. F. Pouget. Mixed experimental and numerical approach for characterizing the biomechanical response of the human leg under elastic compression. *Journal of Biomechanical Engineering*, 132(3), 2010. ISSN 01480731. doi: 10.1115/1.4000967.

B. E. Baker, E. VanHanswyk, S. P. Bogosian, F. W. Werner, and D. Murphy. The effect of knee braces on lateral impact loading of the knee. *American Journal of Sports Medicine*, 17(2):182–186, 1989. ISSN 03635465. doi: 10.1177/036354658901700207.

R. Bakker. The Effect of Sagittal Plane Mechanics on Anterior Cruciate Ligament Strain During Jump Landing. 2014.

B. D. Beynnon, B. C. Fleming, D. L. Churchill, and D. Brown. The effect of anterior cruciate ligament deficiency and functional bracing on translation of the tibia relative to the femur during nonweightbearing and weightbearing. *American Journal of Sports Medicine*, 31(1):99–105, 2003. ISSN 03635465. doi: 10.1177/03635465030310012801.

L. Blankevoort and R. Huiskes. Validation of a three-dimensional model of the knee. *Journal of Biomechanics*, 29(7):955–961, 1996. ISSN 0021-9290. doi: https://doi.org/10.1016/0021-9290(95)00149-2. URL https://www.sciencedirect.com/science/article/pii/0021929095001492.

L. Blankevoort, J. H. Kuiper, R. Huiskes, and H. J. Grootenboer. Articular contact in a three-dimensional model of the knee. *Journal of Biomechanics*, 24(11):1019–1031, 1991. ISSN 00219290. doi: 10.1016/0021-9290(91)90019-J.

K. Cassidy. Design and Validation of a Dynamic Knee Injury Simulator. 2009.

P. W. Cawley, E. P. France, and L. E. Paulos. bracing. pages 226–233.

P. W. Cawley, E. P. France, and L. E. Paulos. Comparison of rehabilitative knee braces. A biomechanical investigation. *American Journal of Sports Medicine*, 17(2):141–146, 1989. ISSN 03635465. doi: 10.1177/036354658901700201.

N. Chandrashekar, J. Slauterbeck, and J. Hashemi. Sex-based differences in the anthropometric characteristics of the anterior cruciate ligament and its relation to intercondylar notch geometry: A cadaveric study. *American Journal of Sports Medicine*, 33(10):1492–1498, 2005. ISSN 03635465. doi: 10.1177/0363546504274149.

B. J. Daley, J. L. Ralston, T. D. Brown, and R. A. Brand. A parametric design evaluation of lateral prophylactic knee braces. *Journal of Biomechanical Engineering*, 115(2):131–136, 1993. ISSN 15288951. doi: 10.1115/1.2894112.

A. Deacon, K. Crossley, P. Brukner, K. Bennell, and Z. S. Kiss. Osteoarthritis of the knee in retired, elite australian rules footballers. *Medical Journal of Australia*, 166(4):187–190, 1997. doi: 10.5694/j.1326-5377.1997.tb140072.x.

E. R. Draper, J. M. Cable, J. Sanchez-Ballester, N. Hunt, J. R. Robinson, and R. K. Strachan. Improvement in function after valgus bracing of the knee. *Journal of Bone and Joint Surgery - Series B*, 82(7):1001–1005, 2000. ISSN 0301620X. doi: 10.1302/0301-620X.82B7.10638.

A. R. Erickson, K. Yasuda, B. Beynnon, R. Johnson, and M. Pope. An in vitro dynamic evaluation of prophylactic knee braces during lateral impact loading. *American Journal of Sports Medicine*, 21(1):26–35, 1993. ISSN 03635465. doi: 10.1177/036354659302100105.

J. C. Gardiner, J. A. Weiss, and T. D. Rosenberg. Strain in the human medial collateral ligament during valgus loading of the knee. *Clinical Orthopaedics and Related Research*, 391(391):266–274, 2001. ISSN 15281132. doi: 10.1097/00003086-200110000-00031.

S. Gerami, M. mousavibaygei, F. Haghi, and F. Pelarak. Anterior cruciate ligament (acl) injuries: A review on the newest reconstruction techniques. *Journal of Family Medicine and Primary Care*, 11(3):852, 2022. doi: 10.4103/jfmpc.jfmpc_1227_21.

G. Hangalur. Effects of Knee Brace on Anterior Cruciate Ligament Strain During Drop-Landing. 2014.

G. Hangalur, E. Brenneman, M. Nicholls, R. Bakker, A. Laing, and N. Chandrashekar. Can a knee brace reduce the strain in the anterior cruciate ligament? A study using combined in vivo/in vitro method. *Prosthetics and Orthotics International*, 40(3):394–399, 2016. ISSN 17461553. doi: 10.1177/0309364615574167.

J. T. Hansen. *Netter's Clinical Anatomy*. Netter Basic Science. Elsevier - Health Sciences Division, Philadelphia, PA, 5 edition, Feb. 2022.

A. Haris and V. Beng Chye Tan. Effectiveness of bilateral single-hinged knee bracing in osteoarthritis: A finite element study. *Proceedings of the Institution of Mechanical Engineers, Part H: Journal of Engineering in Medicine*, 235(8):873–882, 2021. ISSN 20413033. doi: 10.1177/09544119211012493.

H. F. Hart, N. J. Collins, D. C. Ackland, S. M. Cowan, M. A. Hunt, and K. M. Crossley. Immediate Effects of a Brace on Gait Biomechanics for Predominant Lateral Knee Osteoarthritis and Valgus Malalignment after Anterior Cruciate Ligament Reconstruction. *American Journal of Sports Medicine*, 44(4):865–873, 2016. ISSN 15523365. doi: 10.1177/0363546515624677.

J. Hashemi, R. Breighner, T. H. Jang, N. Chandrashekar, S. Ekwaro-Osire, and J. R. Slauterbeck. Increasing pre-activation of the quadriceps muscle protects the anterior cruciate ligament during the landing phase of a jump: An in vitro simulation. *Knee*, 17(3):235–241, 2010. ISSN 09680160. doi: 10.1016/j.knee.2009.09.010. URL http://dx.doi.org/10.1016/j.knee.2009.09.010.

T. L. Haut Donahue, M. L. Hull, M. M. Rashid, and C. R. Jacobs. A finite element model of the human knee joint for the study of tibio-femoral contact. *Journal of Biomechanical Engineering*, 124(3):273–280, 2002. doi: 10.1115/1.1470171.

T. E. Hewett, G. D. Myer, K. R. Ford, M. V. Paterno, and C. E. Quatman. Mechanisms, prediction, and prevention of ACL injuries: Cut risk with three sharpened and validated tools. *Journal of Orthopaedic Research*, 34(11):1843–1855, 2016. ISSN 1554527X. doi: 10.1002/jor.23414.

J. Hewlett and J. Kenney. Innovations in functional and rehabilitative knee bracing. *Annals of Translational Medicine*, 7(S7):S248–S248, 2019. ISSN 23055839. doi: 10.21037/atm.2019.03.34.

J. Hwan Ahn, S. Hak Lee, S. Hee Choi, J. Ho Wang, and S. Won Jang. Evaluation of clinical and magnetic resonance imaging results after treatment with casting and bracing for the acutely injured posterior cruciate ligament. *Arthroscopy: The Journal of Arthroscopic Related Surgery*, 27(12):1679–1687, 2011. ISSN 0749-8063. doi: https://doi.org/10.1016/j.arthro.2011.06.030. URL https://www.sciencedirect.com/science/article/pii/S0749806311006190.

Y. B. Jung, S. K. Tae, Y. S. Lee, H. J. Jung, C. H. Nam, and S. J. Park. Active non-operative treatment of acute isolated posterior cruciate ligament injury with cylinder cast immobilization. *Knee Surgery, Sports Traumatology, Arthroscopy*, 16(8):729–733, 2008. doi: 10.1007/s00167-008-0531-0.

A. Kiapour, A. M. Kiapour, V. Kaul, C. E. Quatman, S. C. Wordeman, T. E. Hewett, C. K. Demetropoulos, and V. K. Goel. Finite element model of the knee for investigation of injury mechanisms: development and validation. *Journal of biomechanical engineering*, 136(1):011002, 2014.

T. Krosshaug, J. R. Slauterbeck, L. Engebretsen, and R. Bahr. Biomechanical analysis of anterior cruciate ligament injury mechanisms: Three-dimensional motion reconstruction from video sequences. *Scandinavian Journal of Medicine amp; Science in Sports*, 17(5):508–519, 2006. doi: 10.1111/j.1600-0838.2006.00558.x.

R. F. LaPrade, S. D. Smith, K. J. Wilson, and C. A. Wijdicks. Quantification of functional brace forces for posterior cruciate ligament injuries on the knee joint: an in vivo investigation. *Knee Surgery, Sports Traumatology, Arthroscopy*, 23(10):3070–3076, 2015. ISSN 14337347. doi: 10.1007/s00167-014-3238-4.

M. A. LeRoux and L. A. Setton. Experimental and biphasic fem determinations of the material properties and hydraulic permeability of the meniscus in tension1. *Journal of Biomechanical Engineering*, 124(3):315–321, 2002. doi: 10.1115/1.1468868.

C. F. Lin, H. Liu, W. E. Garrett, and B. Yu. Effects of a knee extension constraint brace on selected lower extremity motion patterns during a stop-jump task. *Journal of Applied Biomechanics*, 24(2):158–165, 2008. ISSN 15432688. doi: 10.1123/jab.24.2.158.

M. Majewski, H. Susanne, and S. Klaus. Epidemiology of athletic knee injuries: A 10-year study. *Knee*, 13(3):184–188, 2006. ISSN 09680160. doi: 10.1016/j.knee.2006.01.005.

S. G. McLean, Y. K. Oh, M. L. Palmer, S. M. Lucey, D. G. Lucarelli, J. A. Ashton-Miller, and E. M. Wojtys. The relationship between anterior tibial acceleration, tibial slope, and ACL strain during a simulated jump landing task. *Journal of Bone and Joint Surgery*, 93(14):1310–1317, 2011. ISSN 15351386. doi: 10.2106/JBJS.J.00259.

S. J. Meyer, T. D. Brown, D. Ph, M. L. Jimenez, J. E. V. Hoeck, and D. D. Anderson. Benchtop Mechanical Performance of Prophylactic Knee Braces Under Dynamic Valgus Loading: A Cadaver Study. *The Iowa Orthopaedic Journal*, 9(May):92, 1989.

G. D. Myer, K. R. Ford, S. L. Di Stasi, K. D. Barber Foss, L. J. Micheli, and T. E. Hewett. High knee abduction moments are common risk factors for patellofemoral pain (PFP) and anterior cruciate ligament (ACL) injury in girls: Is PFP itself a predictor for subsequent ACL injury? *British Journal of Sports Medicine*, 49(2):118–122, 2015. ISSN 14730480. doi: 10.1136/bjsports-2013-092536.

S. Najibi and J. P. Albright. The use of knee braces, part 1: Prophylactic knee braces in contact sports. *American Journal of Sports Medicine*, 33(4):602–611, 2005. ISSN 03635465. doi: 10.1177/0363546505275128.

L. R. Osternig and R. N. Robertson. Effects of prophylactic knee bracing on lower extremity joint position and muscle activation during running. *The American Journal of Sports Medicine*, 21(5):733–737, 1993. ISSN 15523365. doi: 10.1177/036354659302100518.

L. E. Paulos, P. W. Cawley, and E. P. France. Impact biomechanics of lateral knee bracing: The anterior cruciate ligament. *The American Journal of Sports Medicine*, 19(4):337–342, 1991. ISSN 15523365. doi: 10.1177/036354659101900403.

W. Petersen and T. Zantop. Anatomy of the anterior cruciate ligament with regard to its two bundles. *Clinical Orthopaedics and Related Research*, 454:35–47, 2007. doi: 10.1097/blo.0b013e31802b4a59.

B. Pierrat, J. Molimard, L. Navarro, S. Avril, P. Calmels, and P. Edouard. Efficiency of knee braces: A biomechanical approach based on computational modeling. *ASME 2012 11th Biennial Conference on Engineering Systems Design and Analysis, ESDA 2012*, 4: 237–246, 2012. doi: 10.1115/ESDA2012-82451.

B. Pierrat, J. Molimard, L. Navarro, S. Avril, and P. Calmels. Evaluation of the mechanical efficiency of knee orthoses: A combined experimental-numerical approach. *Proceedings of the Institution of Mechanical Engineers, Part H: Journal of Engineering in Medicine*, 228(6):533–546, 2014. ISSN 20413033. doi: 10.1177/0954411914533944.

B. Pierrat, J. Molimard, L. Navarro, S. Avril, and P. Calmels. Evaluation of the mechanical efficiency of knee braces based on computational modeling. *Computer Methods in Biomechanics and Biomedical Engineering*, 18(6):646–661, 2015a. ISSN 14768259. doi: 10.1080/10255842.2013.832227. URL https://doi.org/10.1080/10255842.2013.832227.

B. Pierrat, J. Molimard, L. Navarro, S. Avril, and P. Calmels. Evaluation of the mechanical efficiency of knee braces based on computational modeling. *Computer Methods in Biomechanics and Biomedical Engineering*, 18(6):646–661, 2015b. ISSN 14768259. doi: 10.1080/10255842.2013.832227. URL https://doi.org/10.1080/10255842.2013.832227.

A. M. Polak. ACL Strain During Single-Leg Jump Landing : An Experimental and Computational Investigation (MASc Thesis). 2019.

F. E. Pollo, J. C. Otis, S. I. Backus, R. F. Warren, and T. L. Wickiewicz. Reduction of medial compartment loads with valgus bracing of the osteoarthritic knee. *American Journal of Sports Medicine*, 30(3):414–421, 2002. ISSN 03635465. doi: 10.1177/03635465020300031801.

B. T. Raines, E. Naclerio, and S. L. Sherman. Management of anterior cruciate ligament injury. *Indian Journal of Orthopaedics*, 51(5):563–575, 2017. doi: 10.4103/ortho.ijortho_245_17.

D. K. Ramsey, M. Lamontagne, P. F. Wretenberg, A. Valentin, B. Engström, and G. Németh. Assessment of functional knee bracing: An in vivo three-dimensional kinematic analysis of the anterior cruciate deficient knee. *Clinical Biomechanics*, 16(1):61–70, 2001. ISSN 02680033. doi: 10.1016/S0268-0033(00)00065-6.

D. K. Ramsey, P. F. Wretenberg, M. Lamontagne, and G. Németh. Electromyographic and biomechanic analysis of anterior cruciate ligament deficiency and functional knee bracing.

Clinical Biomechanics, 18(1):28–34, 2003. ISSN 02680033. doi: 10.1016/S0268-0033(02)00138-9.

H. R. Rao. Computational Modelling of Knee Tissue Mechanics During Single-Leg Jump Landing. Technical report, 2020.

J. D. Richards, J. Sanchez-Ballester, R. K. Jones, N. Darke, and B. N. Livingstone. A comparison of knee braces during walking for the treatment of osteoarthritis of the medial compartment of the knee. *Journal of Bone and Joint Surgery - Series B*, 87(7):937–939, 2005. ISSN 0301620X. doi: 10.1302/0301-620X.87B7.16005.

R. Schween, D. Gehring, and A. Gollhofer. Immediate effects of an elastic knee sleeve on frontal plane gait biomechanics in knee osteoarthritis. *PLoS ONE*, 10(1):1–11, 2015. ISSN 19326203. doi: 10.1371/journal.pone.0115782.

F. Shuaib, D. Kimbrough, M. Roofe, G. McGwin Jr, and P. Jolly. Timing sequence of multi-planar knee kinematics revealed by physiologic cadaveric simulation of landing: Implications for ACL injury mechanism. *Clinical Biomechanics*, 23(1):1–7, 2014. ISSN 15378276. doi: 10.1016/j.clinbiomech.2013.10.017.Timing.

B. Sonnery-Cottet and P. Colombet. Partial tears of the anterior cruciate ligament. *Orthopaedics amp; Traumatology: Surgery amp; Research*, 102(1), 2016. doi: 10.1016/j.otsr.2015.06.032.

S. Srinivasan and Sujatha. Low-dimensional modeling and analysis of human gait with application to the gait of transtibial prosthesis users [electronic resource] /. 11 2022.

Stoko. Stoko support verification. *Paper Knowledge . Toward a Media History of Documents*, 3(April):49–58, 2015.

D. Vlad and M. Oleksik. Research regarding uniaxial tensile strength of nylon woven fabrics, coated and uncoated with silicone. In *MATEC Web of Conferences*, volume 290, page 09003. EDP Sciences, 2019.

T. J. Withrow, L. J. Huston, E. M. Wojtys, and J. A. Ashton-Miller. The relatioship between quadriceps muscle force, knee flexion, and anterior cruciate ligament strain in an in vitro simulated jump landing. *American Journal of Sports Medicine*, 34(2):269–274, 2006. ISSN 03635465. doi: 10.1177/0363546505280906.

W. R. Yu, T. J. Kang, and K. Chung. Drape simulation of woven fabrics by using explicit dynamic analysis. *Journal of the Textile Institute*, 91(2):285–301, 2000. ISSN 17542340. doi: 10.1080/00405000008659507.